Response to Dr. Cyril Brunner

We thank Dr. Brunner for his careful reading and review of our paper. Our detailed responses to his comments follow. Reviewer comments are in blue, our responses are in black, and our corresponding revisions in the manuscript are in red.

General comments:

The authors present a very interesting study on the effect of marine organic aerosol (MOA) on mixed-phase clouds. In particular, they present and validate results from three different MOA emissions schemes, quantify the resulting spatial cloud condensation nuclei and ice nucleating particles (INP) number concentrations and compare it to modeled INP concentrations of dust, using state of the art parametrizations. In contrast to previous work by other authors, they present data comparing the INP population of MOA to INPs of dust.

The writing (from an editorial standpoint) is to be commended. The methodology is stringent and valid. The assumptions made are to a majority stated and their impact on the result comprehensibly assessed. The work addresses relevant scientific atmospheric questions with impacts on global climate simulations. The topic of the paper is well suited for ACP. I recommend the manuscript for publication if the following minor comments are addressed:

We thank the reviewer for the encouraging comments. We have revised the manuscript following your comments and clarified the text to improve the paper.

Specific comments:

Page 2 (line 12/13). I do not fully understand why the three regions are stated. Are mixed-phase clouds only observed in the Arctic, Antarctic, and over the Southern Ocean? As the paper is also not focusing on these regions, I would propose to rephrase the sentence. E.g., include all regions or specify what is unique about mixed-phase clouds in the three stated regions.

We thank the reviewer for the suggestion. We have revised the sentence to read:

"Mixed-phase clouds are frequently observed in high-latitude regions, and..."

Page 3 (lines 44-48). Kanji et al, 2017 provide an excellent overview of the different modes of freezing. The stated mechanism, however, was not introduced by Kanji et al., 2017. Please cite the original source or e.g. Vali, G., DeMott, P. J., Möhler, O., andWhale, T. F.: Technical Note: A proposal for ice nucleation terminology, Atmos. Chem.Phys., 15, 10263–10270, https://doi.org/10.5194/acp-15-10263-2015, 2015.

We thank the reviewer for the suggestion. We have added the reference as you suggested, and the revised sentence reads as:

"In mixed-phase clouds in which air temperature is between –38˚ C and 0˚ C, ice is initialized only by heterogeneous nucleation on ice nucleating particles (INPs) (Vali et al., 2015)."

Page 15 (line 399). Is for the NULL approach the annual global MOA or sea salt emission 4.6 Tg yr-1? Please specify.

We thank the reviewer for the suggestion. We meant the annal global MOA emission of 4.6 Tg yr^{-1}. We have revised the sentence as:

"The NULL approach only gives an annual global MOA emission of 4.6 Tg yr^{-1}".

Page 23/24 (lines 652-683). The missing representation of secondary ice formation is nicely formulated. However, the study also does not model other IN species, such as ash, biomass-burning particles, or other land-borne bio particles. Please elaborate on the impact of this (valid) simplification on the study's results.

We thank the reviewer for the excellent comment. We have added some discussion on missing representation of other types of INPs in the model in the newly added third paragraph of section 4. The revised sentences read as:

"In this study, other potential INP species than dust and MOA, such as ash, biomass-burning particles, or other land-borne biological particles (Hoose et al., 2010; Jahn et al., 2020; Schill et al., 2020) are not represented in the model. These INP species can be regionally important at certain temperature regimes of mixed-phase clouds. Accounting for these species may increase the INP concentrations predicted in the model and change the mixed-phase cloud properties, particularly at warmer temperatures > -15ºC. The impacts of these INP species will be quantified in our future studies."

Page 32 (Table 1). Please explain variables in the caption, such as g, to support the reader's quicker understanding.

We thank the reviewer for the suggestion. We have added the explanations for variables in Table 1, and the revised caption for Table 1 reads:

Table 1. Aerosol species in MAM4 modes

	Accumulation	Aitken	Coarse	Primary Carbon
Species[1]	num_a1, so4_a1, pom_a1, soa_a1, bc_a1, dst_a1, ncl_a1, moa_a1	num_a2, so4_a2, soa_a2, ncl_a2, dst_a2, moa_a2	num_a3, dst_a3, ncl_a3, so4_a3	num_a4, pom_a4, bc_a4, (moa_a4 if externally mixed)
Size range	0.08 – 1 μm	0.02 – 0.08 μm	1–10 μm	0.08 – 1 μm
Standard Deviation σg	1.6	1.6	1.2	1.6
Number-median diameter *Dgn*	1.1×10^{-7}	2.6×10^{-8}	2.0×10^{-6}	5.0×10^{-8}
Low bound *Dgn*	5.35×10^{-8}	8.7×10^{-9}	4.0×10^{-7}	1.0×10^{-8}
High bound *Dgn*	4.8×10^{-7}	5.2×10^{-8}	4.0×10^{-5}	1.0×10^{-7}

[1]so4_aX: sulfate mass mixing ratio in mode X; pom_aX: particulate organic matter (POM) mass mixing ratio in mode X; soa_aX: secondary organic aerosol (SOA) mass mixing ratio in mode X; bc_aX: black carbon (BC) mass mixing ratio in mode X; dst_aX: dust mass mixing ratio in mode X; ncl_aX: sea salt mass mixing ratio in mode X; moa_aX: marine organic aerosol (MOA) mass mixing ratio in mode X; and num_aX: number mixing ratio of mode X. *_a1: accumulation mode; *_a2: Aitken mode; *_a3: coarse mode; and *_a4: coarse mode.

Page 46 (Figure 6). No need to change anything, just a general comment. With INP measurements, we are often divided about how the show the INP concentration most representatively over a long period. If we calculate the mean concentration, the result will be "biased" towards higher INP concentrations if a few events with INP concentrations in the order of 102 to 103 are present. IMHO showing presenting the reader also with the median concentration provides a complete picture.

We thank the reviewer for the suggestion. We agree with the reviewer that mean concentration will be "biased" towards the higher INP. However, in GCMs we are simulating the climatological states of aerosols, not episodical events.

Supplement (Figure S1). The unit of plot d) is not fully visible

Thanks. We have fixed this. The revised Figure looks like:

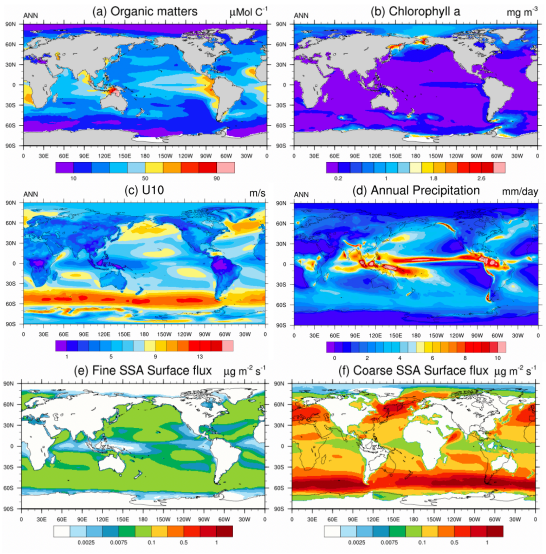
(a) Organic matters
µMol C-1
ANN
(b) Chlorophyll a
mg m-3
ANN
(c) U10
m/s
ANN
(d) Annual Precipitation
mm/day
ANN
(e) Fine SSA Surface flux
µg m-2 s-1
(f) Coarse SSA Surface flux
µg m-2 s-1

Response to reviewer 2

We thank the anonymous reviewer for the careful review and constructive comments on our manuscript. Our responses to individual comments follow. Reviewer comments are in blue, our responses are in black, and our corresponding revisions in the manuscript are in red.

The manuscript titled: "Effects of Marine Organic Aerosols as Sources of Immersion Mode Ice Nucleating Particles on High Latitude Mixed-Phase Clouds" discusses the impacts of adding marine organic aerosols (MOA) into the Community Atmosphere Model (version 6) on cloud properties. The study shows that introducing MOA as an aerosol species leads to a higher concentration of available CCN and INP, which results in different cloud properties. In contrast to the title of the study, the authors find that MOA has a much larger effect on the CCN concentration and related cloud radiative forcing, relative to INP and associated cloud radiative forcing. Nevertheless, the study does show that adding MOA increases the number of INPs and that MOA-INP are likely the most important INP species over the Southern Ocean, especially at heights below 400 hPa. I would like to commend the authors on a very well written and thorough study. However, I found the implementation of the emission scheme quite confusing and vague. I also have some additional comments below.

We thank the reviewer for the constructive comments, which greatly improve the clarity of our paper. In this study, as the title indicates, we focus on the MOA INP effects, since earlier studies (Meskhidze et al., 2011; Gantt et al., 2012; Burrow et al., 2018), using earlier versions of CAM, have investigated the MOA CCN effects. As the reviewer correctly indicates, INP effects of MOA on cloud properties and radiative forcing can be regionally strong in remote marine environments such as over the Southern Ocean.

We have significantly revised the method section of our manuscript to improve its clarity related to the emission scheme.

General comments:

In regards to the implementation of the MOA emission, it is not very clear how the MOA particles are handled. Firstly, how is the mixing state of the MOA determined (i.e. internally or externally mixed)? Does this just depend on the size mode of the emitted sea salt aerosol? If yes, how does the mass of the emitted MOA impact the resulting size of the sea salt and therefore the mixing state. Secondly, for the externally mixed MOA, how is the size versus number determined? Perhaps I am completely misunderstanding how this is done but please clarify in the methods.

We thank the reviewer for the suggestion. In the following, we will clarify the confusing points one by one.

Firstly, regarding the mixing state of the MOA: MAM in CAM6 adopts the modal approach, where aerosol species are assumed to be internally mixed within a mode, and externally mixed between modes. MOA is emitted into the fine aerosol modes with different assumptions of mixing state with inorganic sea salt: (1) MOA is emitted into the Aitken and accumulation modes together with sea salt in the case of internally mixed with sea salt; or (2) MOA is emitted into the Aitken and primary

carbon mode separately from sea salt in the case of externally mixed with sea salt. MOA is not emitted into the coarse mode though sea salt does. In addition, there is another assumption of whether the experimentally derived parameterizations of sea spray aerosol mass emission flux represent the total emission of MOA and sea salt or only account for the emission of sea salt. In the former case, MOA will *replace* the mass and number emission fluxes of sea salt. In the latter case, MOA will *add* onto both the sea salt mass and number emission fluxes. Burrows et al. (2018) tested different combinations of the two assumptions and found that the "internally-mixed" and "added" approach for MOA provides the most physically realistic configuration compared to the observations. Thus, we used this configuration in our study. In this configuration, the emission of MOA will not impact the emission fluxes of sea salt. We acknowledge that current experiments and observations do not provide precise constrains on the mixing state. For the impacts of different assumption of mixing state we refer the readers to Burrows et al. (2018).

Second, the emitted MOA mass flux is calculated as:

$$F_{MOA/SSA} = \frac{M_{MOA}}{M_{sea\ spray}} = \frac{M_{MOA}}{M_{MOA} + M_{sea\ salt}}$$

where $F_{MOA/SSA}$ is the mass fraction of MOA in total SSA. G11, B14, and NULL emission schemes are used to calculate $F_{MOA/SSA}$, respectively. $M_{sea\ salt}$ is the emitted sea salt mass, calculated following the parameterization of Mårtensson et al. (2003) for dry particle diameters from 0.020 to 2.8 μm, and Monahan et al. (1986) from 2.8 to 10 μm in the model.

Third, the emitted MOA number flux is calculated based on the emitted MOA mass flux for a given particle diameter within the emission size range (from 0.020 to 2.8 μm) of the Mårtensson et al. parameterization, and the particle density of MOA, the latter of which is set to be 1601 kg m^{-3}, as given in Table 2.

In response to the comments made by reviewers, we revised the manuscript:

We added some discussions on the mixing state of aerosol in Section 2.1:

"MAM in CAM6 adopts the modal approach, where aerosol species are assumed to be internally mixed within a mode, and externally mixed between modes. MOA is emitted into the fine aerosol modes with different assumptions of mixing state with inorganic sea salt: (1) MOA is emitted into the Aitken and accumulation modes together with sea salt in the case of internally mixed with sea salt; or (2) MOA is emitted into the Aitken and primary carbon mode separately from sea salt in the case of externally mixed with sea salt. In addition, there is another assumption of whether the experimentally derived parameterizations of SSA mass emission flux represent the total emission of MOA and sea salt or only account for the emission of sea salt. In the former case, MOA will *replace* the mass and number emission fluxes of sea salt. In the latter case, MOA will *add* onto the sea salt mass and number emission fluxes. Burrows et al. (2018) tested different combinations of the two assumptions and found that the "internally-mixed" and "added" MOA approach provides the most physically

realistic configuration compared to the observations. Thus, in our study we use this configuration but acknowledge that current observations do not provide precise constrains on the mixing state."

The discussion of emitted MOA number mixing ratio is added in Section 2.2.1 of the revised manuscript:

"The MOA number emission flux is calculated based on the MOA mass emission flux for a given particle diameter within the emission size range (from 0.020 to 2.8 μm for the Mårtensson et al. parameterization) and particle density of MOA, the latter of which is set to be 1601 kg m^{-3} (Liu et al., 2012), as given in Table 2."

When considering the internally mixed MOA with sea salt, is a freezing point depression considered when using the ice nucleation parametrizations? Based on the mass fractions of MOA relative to sea salt for the majority of the particles, sea salt appears to be the dominant component of the aerosol and I expect this to significantly lower the freezing efficiency of the MOA.

We thank the reviewer for the good suggestion. The M18 ice nucleation scheme is derived based on the correlation between ambient sea spray aerosols and INPs measured by the Count-Flow Diffusion Chamber (CFDC) during the "clean scenario" at Mace Head. This means that this parameterization has already accounted for the freezing point depression effect when MOA INPs in droplets induce freezing in CFDC. The W15 scheme is developed based on laboratory measurements of immersion-freezing of materials aerosolized from sea surface microlayer samples collected in the N. Atlantic and Arctic Oceans. Thus, this parameterization should have also accounted for the freezing point depression effect during the freezing of droplets induced by MOA.

How does the lower hygroscopicity of the MOA relative to sea salt, factor into the available CCN numbers? Perhaps this will become clearer once the number and size of the MOA and its mixing state is explained more clearly.

We thank the reviewer for this question. The hygroscopicity of the MOA is 0.1, compared with 1.16 of sea salt, as listed in Table 2. In our reply to your comment above, MOA is assumed to be internally mixed with sea salt in the accumulation and Aitken modes in this study. The hygroscopicity of aerosols in a mode is calculated based on volume-averaged hygroscopicities of all aerosol species in the mode and used in the aerosol activation calculation. After considering MOA in the model, the mode volume-averaged hygroscopicity is reduced compared to pure sea salt aerosol. However, number concentrations of CCN are still increased with the "added" MOA into the model.

We added the following sentence in Section 2.2 of the revised manuscript:

"The mode volume-averaged hygroscopicity is reduced due to lower hygroscopicity of MOA. However, based on the method to calculate sea salt emission (Liu et al., 2012) for a given aerosol mode, the "added" MOA mass increases the number concentrations of aerosols in the Aitken and accumulation modes, which overcomes the reduction in mode hygroscopicity to activate more CCN."

A major point of the paper is that the addition of MOA greatly improves the representation of INP over the Southern Ocean and to some extent over the Arctic. However, when looking at the comparisons to the field observations, it could be argued that the N12 scheme does better at predicting observed INP concentrations. Therefore, perhaps it is better to compare the influence of adding MOA as an INP to the N12 scheme. I understand that this comparison will not be as straightforward but it seems a bit unfair to say that MOA is an important INP by comparing to D15, which clearly underestimates the observed INP concentrations and as the authors mention, only considers dust particles larger than 500 nm. Nevertheless, I support the author's conclusion that MOA is likely an important INP species over remote regions such as the Southern Ocean. However, I think comparing to D15 may be making MOA out to be more important than it is.

We thank the reviewer for the good comment. It seems that the N12 scheme has the better performance than D15 in Figure 4. However, the field campaigns used in Figure 4 are marine aerosol dominant/contained scenario campaigns. MOA is identified as an important INP source during these campaigns from measurements (McCluskey, Ovadnevaite, Rinaldi, et al., 2018b; McCluskey, Hill, Humphries, et al., 2018a). For example, CAPRICORN and SOCRATES, these two campaigns were conducted over the Southern Ocean where dust aerosol was less influenced. The "clean scenario" (McCluskey, Ovadnevaite, Rinaldi, et al., 2018b) during the Mace Head campaign is selected to focus on marine aerosol influence. Thus, dust should not be expected to be the dominant INPs as indicated by the N12 scheme which only considers dust INPs. This suggests that N12 may overestimate dust INPs. This is also confirmed in our previous study (Shi and Liu, 2019) which compared the D15 and N12 schemes with the field observations conducted in the Arctic subject to the major influence from dust. It was found that D15 underestimates the observed INPs while N12 has a better performance. However, the host aerosol-climate model was found to significantly underestimate the observed dust concentrations by up to a factor of 10 due to missing local Arctic sources and too weak transport of dust from low latitudes. Considering the low bias of dust in the Arctic predicted by the host model, that study suggested that D15 overall has the better performance in representing dust INPs.

To improve the clarity, we revised the experiment description in section 2.3 of the revised manuscript as

"The control experiment (CTL) is the same as BASE except that the D15 dust ice nucleation scheme was used to replace the CNT scheme in BASE, because D15 gave a better model performance compared with observations in our previous study (Shi and Liu, 2019)."

We added in section 3.3 of the revised manuscript:

"The N12 scheme has the better performance than D15 in Figure 4. However, the field campaigns used in Figure 4 are marine aerosol dominant/contained scenario campaigns. MOA is identified as an important INP source during these campaigns from measurements (McCluskey, Ovadnevaite, Rinaldi, et al., 2018b; McCluskey, Hill, Humphries, et al., 2018a). Thus, dust should not be expected to be the dominant INPs as indicated by the N12 scheme which only considers dust INPs. This suggests that N12 may overestimate dust INPs, which is consistent with our earlier study (Shi and Liu, 2019)."

As the Southern Ocean is where the largest changes in INP and CCN are observed, I find it quite surprising how little mention there is of sea ice extent. In theory, and to some degree is seems like some of the reported values in the study show this, the emission of MOA should be greatly reduced during the austral winter and early spring. In fact, I think the handling of sea ice in the model should be more clearly discussed and the seasonal influence on emission of MOA would warrant its own figure (perhaps in the supplement).

We agree with the reviewer that sea ice has a significant influence on the emission of MOA. As shown in Figure 2a, MOA concentrations are higher in January (austral summer) and lower in July (austral winter) at Amsterdam Island in the Southern Hemisphere, which reflects the seasonal change of MOA emissions.

In this study, all experiment is set up using "F2000climo" component in CESM2-CAM6 model. As described in section 2.3, "All simulations were performed for 10 years with prescribed climatological sea surface temperatures and sea ice." The atmosphere model is not coupled with the sea ice model, but uses the prescribed climatological sea ice as its boundary condition. The sea ice data has a seasonal variation, namely, it has 12 months as a time dimension. The sea ice extent will impact the seasonal variation of MOA emission.

Following the reviewer's comment, we added a figure in the supplement showing the seasonal variation of sea ice extent and related discussion on the impact of sea ice extent on the emission of MOA in the revised manuscript in section 3.1:

"The sea ice extent prescribed in the model as a boundary condition has a strong seasonal variation over the Southern Ocean, as shown in supplementary Figure S2. This can greatly impact the emission of MOA there (e.g., low emission during the austral winter and early spring)."

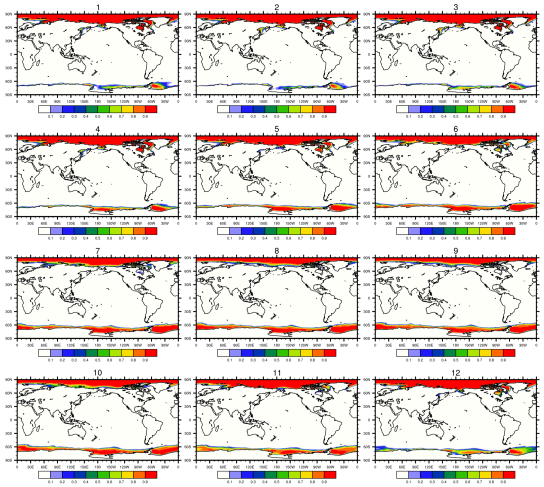

Figure S2. Seasonal variation of global sea ice extent, shown as sea ice fraction in 12 months.

Minor comments:

Line 186-192: As I am not so familiar with MAM4, it is unclear to me where the SSA aerosol falls into one of the six aerosol species? Does it count as sea salt and are the cited parametrization used to determine the size distribution of sea salt?

In this study, the sea spray aerosol (SSA) refers to sea salt plus MOA. Sea salt is part of SSA. MOA is added into MAM4 as a new species (sea salt is already implemented in MAM4), which means newly predicted variables in MAM4 to trace the temporal and spatial variations of MOA mass mixing ratios. In the "internally-mixed" and "added" MOA approach used in this study, the emitted mass mixing ratio of MOA is dependent on the emission of sea salt mass mixing ratio and the mass fraction of MOA in total SSA, $F_{MOA/SSA}$. The Mårtensson et al. (2003) and Monahan et al. (1986) parameterizations are used to calculate the sea salt emission flux, while the G11, B14, and NULL emission schemes are used to calculate $F_{MOA/SSA}$.

Line 218-223: The G11 scheme requires the input of the chlorophyll concentration. This may show my ignorance but is chlorophyll predicted in the model or is it taken from fixed look up tables? If this comes from look up tables, does it account for seasonal variability and if so, how is the chlorophyll

concentration over the Southern Ocean determined during the austral winter when satellite data for chlorophyll is limited to lower latitudes (below ~55 degrees)?

Thank the reviewer for the comment. We used the prescribed climatological data for chlorophyll concentrations, and this data has a seasonal variation, namely, it has 12 months as the time dimension. Below we plotted the chlorophyll concentrations we used in the model for each month, shown as Figure R1. We noticed much larger values during the austral summer (DJF) than those during the austral winter (JJA) over the Southern Ocean. This is expected since phytoplankton activities are minimal in the austral winter in the Southern Hemisphere high latitudes.

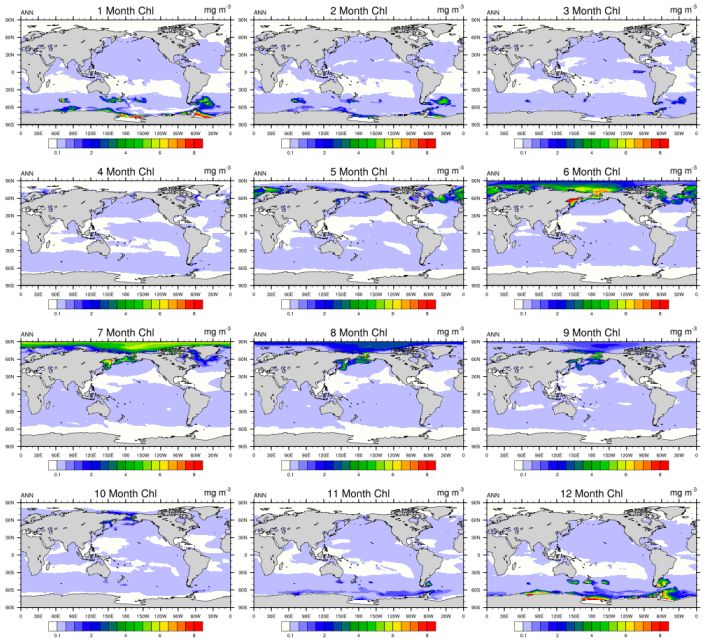

Figure R1. Seasonal variation for global distribution of chlorophyll concentrations.

Section 2.2.2: This section is a bit confusing as it is unclear which method was used here. Is the MOA emitted in the externally-mixed or internally-mixed approach? Based on the authors, it sounds like the Burrows et al, 2018 approach where the MOA is internally mixed should be used. Is that what is done here? If yes, and if the MOA is added to the sea salt fraction, does this not lead to an overall reduction in the hygroscopicity of the sea salt aerosols (or a freezing point depression)? Or is the increase in sea salt mass due to the MOA fraction make the resulting particles large enough to overcome the reduction in hygroscopicity of the particles to act as CCN? Or does the MOA fraction also increase the number of sea salt+MOA particles. If the latter is the case how is the increase in number concentration

handled as the MOA always scales with sea salt mass. Perhaps it would be worthwhile to clarify how the inclusion of the MOA fraction to the different size modes (i.e. Aitken, Accumulation, Coarse, Primary) acts to increase the number and size of the sea salt aerosol and lowers its overall hygroscopicity.

We thank the reviewer for the comments. Following the suggestion of Burrows et al. (2018), we used the "internally-mixed" and "added" approach for MOA in this study. We have made it clear in the revised manuscript. In this "internally-mixed approach" MOA is emitted into the Aitken and accumulation modes along with sea salt.

Yes, the mode averaged hygroscopicity is reduced due to lower hygroscopicity of MOA. However, the "added" MOA mass increases the number concentrations of sea salt+MOA aerosols in the size ranges of the Aitken and accumulation modes, which overcomes the reduction in mode hygroscopicity to activate more CCN.

As documented in Liu et al. (2012), when calculating sea salt emission, sea salt size distribution is divided into many small size bins, where the emission of sea salt mass mixing ratio is calculated based on the Mårtensson et al. (2003) and Monahan et al. (1986) parameterizations, and the emission of sea salt number mixing ratio for a given size bin is derived based on the mass emission. The total mass and number emissions for an aerosol mode are summed up over the relevant size bins. In this study, the "added" MOA number mixing ratio is calculated similarly based on the emitted MOA mass mixing ratio, particle size for a given bin, and the particle density of MOA, as number is proportional to mass for a given size bin. Therefore, after considering MOA in the model, number concentrations of sea salt+MOA in the Aitken and accumulation modes are increased.

To avoid confusion, we revised the MOA emission description in section 2.2.2 of the revised manuscript as

"MOA is emitted into different aerosol modes depending on mixing state of MOA and sea salt (Burrows et al., 2014, 2018). In the internally-mixed emission approach, MOA is emitted into the accumulation and Aitken modes along with sea salt, as shown in Table 1. In contrast, MOA is emitted into the Aitken and primary carbon modes in the externally-mixed emission approach. Furthermore, the emission of MOA can replace or be added to sea salt emission in terms of mass and number in the model. Burrows et al. (2018) found that simulated MOA amounts, seasonal cycles, and impacts on CCN over the Southern Ocean show better agreement with observations under the assumption that emitted MOA is added to, and internally mixed with sea salt. Thus, we used the "internally-mixed" and "added" approach for MOA emission in this study. As shown in Table 2, the hygroscopicity of MOA is set to be 0.1 following Burrows et al. (2014, 2018), compared to 1.16 for sea salt. The mode hygroscopicity is calculated as the volume-weighted average of hygroscopicities of all species in a mode, which is then used in the Abdul-Razzak and Ghan (2000) droplet activation parameterization in CAM6. The mode hygroscopicity is reduced due to lower hygroscopicity of MOA. However, based on the method to calculate sea salt emission (Liu et al., 2012) for a given aerosol mode, the "added" MOA mass increases the number concentrations of particles in the Aitken and accumulation modes, which overcomes the reduction in mode hygroscopicity to activate more CCN."

Table 1: Please explain the names of the aerosol species in MAM4. Perhaps these are standard in the modelling community but would be helpful for the reader to know what the acronyms stand for easily. That being said perhaps the same acronyms can be used in Table 1 and 2 for consistency and easy reference.

Thanks, we have added the explanation of the names of the aerosol species in MAM4. Please note that we use *_aX to indicate aerosol species in mode X (i.e., a1 for accumulation, a2 for Aitken, a3 for coarse, and a4 for primary carbon mode.

Table 1. Aerosol species in MAM4 modes

	Accumulation	**Aitken**	**Coarse**	**Primary Carbon**
Species[1]	num_a1, so4_a1, pom_a1, soa_a1, bc_a1, dst_a1, ncl_a1, moa_a1	num_a2, so4_a2, soa_a2, ncl_a2, dst_a2, moa_a2	num_a3, dst_a3, ncl_a3, so4_a3	num_a4, pom_a4, bc_a4, (moa_a4 if externally mixed)
Size range	0.08 – 1 μm	0.02 – 0.08 μm	1–10 μm	0.08 – 1 μm
Standard Deviation σg	1.6	1.6	1.2	1.6
Number-median diameter *Dgn*	1.1×10^{-7}	2.6×10^{-8}	2.0×10^{-6}	5.0×10^{-8}
Low bound *Dgn*	5.35×10^{-8}	8.7×10^{-9}	4.0×10^{-7}	1.0×10^{-8}
High bound *Dgn*	4.8×10^{-7}	5.2×10^{-8}	4.0×10^{-5}	1.0×10^{-7}

[1]so4_aX: sulfate mass mixing ratio in mode X; pom_aX: particulate organic matter (POM) mass mixing ratio in mode X; soa_aX: secondary organic aerosol (SOA) mass mixing ratio in mode X; bc_aX: black carbon (BC) mass mixing ratio in mode X; dst_aX: dust mass mixing ratio in mode X; ncl_aX: sea salt mass mixing ratio in mode X; moa_aX: marine organic aerosol (MOA) mass mixing ratio in mode X; and num_aX: number mixing ratio of mode X. *_a1: accumulation mode; *_a2: Aitken mode; *_a3: coarse mode; and *_a4: coarse mode.

Table 2. Aerosol species and physical properties

Species	**Name**	**Density (kg m^{-3})**	**Hygroscopicity**
BC	Black carbon	1700	1.0×10^{-10}
SO4	Sulfate	1770	0.507
SOA	Secondary organic	1000	0.14
POA	Primary organic	1000	1.0×10^{-10}
DST	Dust	2600	0.068
NCL	Sea salt	1900	1.16
MOA	Marine organic aerosol	1601	0.1

Section 2.2.2a: Please explain how the TOC is derived for the W15 scheme. Furthermore, is the TOC estimated from the sea surface or derived from the fraction emitted MOA? Later it is stated that it comes from the surface when expalianing why W15 may be overestimating but please add that here.

We thank the reviewer for the suggestion. Yes, the W15 scheme is derived based on TOC in sea surface microlayer samples, which may not be representative of ambient MOA. We added a note in the description of W15 in section 2.2.2a as

"W15 is developed based on the TOC in the sea surface microlayer samples, which may not be representative of ambient MOA."

Section 2.2.2b: Again here is it not immediately clear how this parametrization is implemented. Is this just dependent on temperature or is the MOA fraction somehow utilized here? Is the derived ns value applied to the total surface area and number concentration of the sea spray aerosol to activate a certain number of particles into ice crystals and if so what aerosol size modes are used? Also, how is the freezing point depression handled. Afterall, the particles are primarily composed of sea salt (at least the internally mixed ones)

We thank the reviewer for the suggestion. $n_s(T)$ in Equation (8) is used to calculate MOA INPs based on

$$N_{INP}(T) = N_{tot} S_{ae} n_s(T)$$

where S_{ae} and N_{tot} are the total surface area and number mixing ratio of SSA, calculated for the Aitken and accumulation modes, respectively. M18 is derived based on the correlation between ambient SSA aerosols and INPs during the "clean scenario" at Mace Head Station in August 2015. INPs were measured by CFDC, and thus, should have accounted for the effect of freezing point depression on droplets freezing.

We modified the description of M18 in the section 2.2.2b as

"MOA INP number concentration is then calculated by: $N_{INP}(T) = N_{tot} S_{ae} n_s(T)$, where S_{ae} and N_{tot} are the total surface area and number mixing ratio of SSA, calculated for the Aitken and accumulation modes, respectively."

Line 396-399: How do these studies justify such low fractions of MOA to sea salt when the laboratory studies report much higher fractions of MOA to SSA in the literature previously cited in the paper (ie. Prather et al, 2013 and Facchini et al, 2008) or are the large contributions of other compounds than MOA and sea salt in SSA? Furthermore, when looking at Figure 2, the fraction of MOA in SSA is much of high MOA emission, however it is unclear what SSA emission looks like globally. Perhaps it would be worthwhile to plot MOA/SSA emissions as an addition to Fig. S1.

We thank the reviewer for the comments. The ratios of MOA emission to sea salt emission include the emission of sea salt in the coarse mode, which dominates the total sea salt emission. Figure 2c shows

the simulated and measured mass fraction of MOA in SSA for the Aitken and accumulation modes (MOA is not considered in the coarse mode). We added a note in section 3.1 to make it clearer when we talk about the ratios of MOA emission and sea salt emission. We have shown the MOA emission in Figure 1. Following the reviewer's comment, we added the SSA emissions in fine (Aitken plus accumulation) and coarse modes in Figure S1.

"We note that emissions and burdens of sea salt include the contribution from the coarse mode, which dominates the total sea salt emissions and burdens."

Line 401-406: I find the switch between SSA and sea salt mass rather distracting when discussing the comparison of MOA fractions. Consider making this consistent as to my understanding, SSA is MOA+Sea salt and so it is just a different way of comparing the same values (e.g. MOA/(MOA+Sea salt) or MOA/Sea salt).

We thank the reviewer for the suggestion. We revised the manuscript to make it consistent:

"In B14, the ratio of MOA to sea salt mass burdens reaches up to 2.3 and 1.0 for the Aitken and accumulation modes, respectively. Number concentrations of accumulation mode aerosols near the surface are increased by up to 50% over some regions of the Southern Ocean and Arctic."

Table 5: Perhaps it would be worthwhile to also show the change in mean hygroscopicity of the emitted aerosols as the overall burdens do not seem to change much. Considering some of my comments on section 2.2.2, it would also be worthwhile to see the change in mean number and size of the sea salt and MOA aerosols emitted. I know this greatly varies by region but it would make it clearer to see how adding MOA to the model impacts the number of potential available particles to act as CCN. Also, as previously mentioned, based on the literature discussion, why is the fraction of MOA (MOA/Sea Salt) emission so much lower than reported values of around a few percent for particles larger than 1 micron and even higher for smaller particles?

We thank the reviewer for the suggestion. We are sorry for the confusion and again the numbers for sea salt in Table 5 include the contribution from the coarse mode, while MOA is only contained in the Aitken and accumulation modes. Sea salt burdens in the Aitken and accumulation modes are 0.0014 and 0.48 Tg, respectively, comparing to 8.32 Tg in the coarse mode. We did not output the hygroscopicity, but we have output of number concentrations of aerosols in each mode. Figure R2 shows the change of number concentrations of aerosols in the Aitken and accumulation modes when adding MOA by comparing two model simulations with and without MOA emissions. We notice an increase by up to 50% in the Accumulation mode number concentrations over some regions of the Southern Ocean and Arctic after adding MOA into the model (Figure R2).

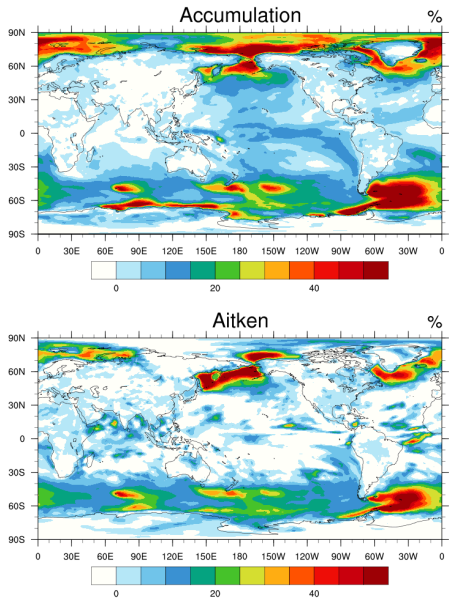

Figure R2. Annual mean global distribution of the change ((N_{B14_D15}-N_{BASE})/N_{BASE}) of number concentrations of aerosols in the Aitken and accumulation modes, calculated from B15_D15 and BASE experiments.

Line 462: Consider revising to state that impact on clouds via CCN will be discussed next as the INP section follows section 3.2

Thanks. The revised sentence reads as

"Next we will study the MOA effects on clouds via acting as CCN (section 3.2) and INPs (section 3.3), based on model experiments with the B14 emission (Table 4)."

Figure 3: Is there a reason why such a decrease is observed over the Tibetan plateau? Is there a way to add hatching for regions where the changes between simulations are significant or are these changes significant because they are the averages over the nine years?

We thank the reviewer for the suggestion. The decrease CCN over Tibetan plateau after adding MOA into the model is not statistically significant. We revised Figure 3 as suggested by adding the hatching for the regions which pass the significance test (at 95% level), shown below

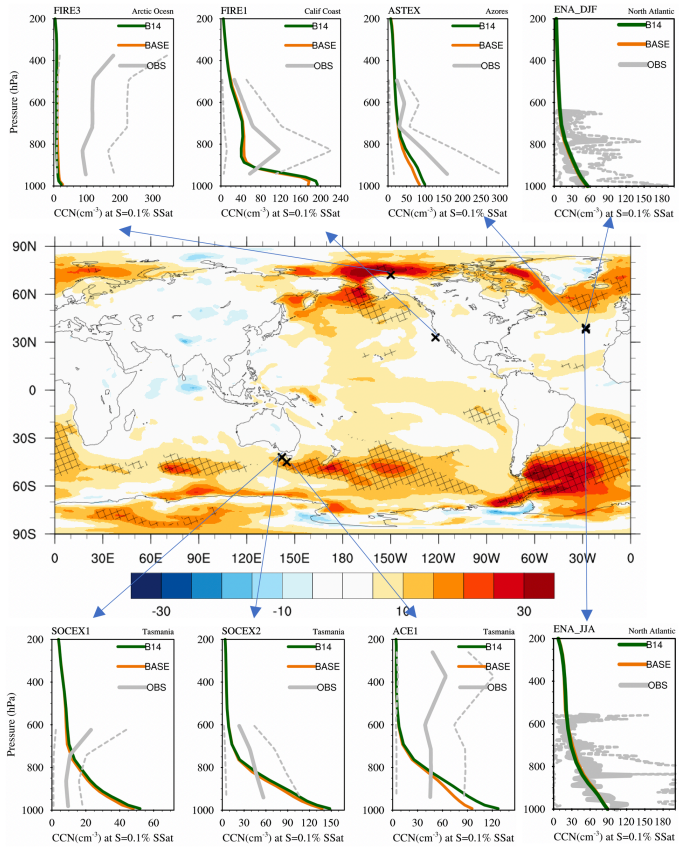

Line 514-515: I would argue that the N12 parametrization does the best job of predicting the INP concentrations across the entire temperature range as shown in Figure 4. This is mischaracterized in these sentences. In fact based on the ability of N12, it would be possible to argue that including MOA emission is not needed to accurately predict the observed INP concentrations.

See our reply to your general comment above. In summary, the field campaigns used in Figure 4 are marine aerosol dominant/contained scenario campaigns. Thus, dust should not be expected to be the dominant INPs as indicated by the N12 scheme which only considers dust. Our previous study (Shi

and Liu, 2019) also showed that N12 predicts much higher INPs than D15 and agrees better with the INP observations in the Arctic subject to major influences of dust. However, the host aerosol-climate model was found to significantly underestimate the observed dust concentrations by up to a factor of 10. If there were no underestimation of modeled dust, dust INP concentrations from N12 would be much higher than observations. Therefore, N12 has overall the best performance for the wrong reason.

Line 521-523: Following up in the previous comment, the fact that combining M18 and D15 still under predicts, shows that the MOA addition is not as good as just using the N12 parametrization. And one could argue that when using the entire size distribution for dust nucleation, the majority of INPs would accurately simulated.

We thank the reviewer for the suggestion. We agree with the reviewer that the result from D15+M18 scheme is not a perfect match with observations, particularly at temperatures warmer than -15 °C. This may indicate that model misses the representation of marine biological aerosols, which are effective INPs at these warmer temperatures. We also note that N12 overestimates observed INPs even at these warmer temperatures.

Figure 5: How are the parametrizations drawn for the flight campaigns (e.g. Socrates), where INP measured aboard the aircraft are sometimes collected at different altitudes? Line 540-551 and Figure 6: Why was INPs at -25 C and 950 hPa used for this analysis here? For cloud formation, this seems highly irrelevant as it is rarely -25 C at 950 hPa especially in the regions where MOA is expected to be important (over ice-free regions of the Ocean). In fact, how common is it for MPCs to exist at this height. This seems like an unfair height for showing the importance of MOA as INPs as it is a height where MOA concentrations are extremely high due to being within the boundary layer and at a temperature where the ability of MOA to freeze is essentially maximized based on field measurement techniques used at temps above ~-30 C.

We thank the reviewer for the suggestion. In Figures 4 and 5, the simulated INP concentrations are sampled at the same altitudes as the observation data, in the case of aircraft observations.

Figure 6 shows the diagnostic INP at -25℃ at 950 hPa. We used model MOA and dust concentrations at 950 hPa as inputs, and diagnosed the INP concentrations at -25℃. This is similar to what the CFDC-based and filter-based methods measure INPs at a given temperature (often at -25℃). As shown in Figure 6d, the importance of MOA INPs versus dust INPs is not highly variable within the marine boundary layer. Following the reviewer's comment, we also diagnose INP concentrations at -10 and -35℃. As shown in Figure R3, the diagnostic INP distribution patterns are similar to that at -25℃, although the magnitude of INP concentrations (for MOA and dust) are changed. Thus our conclusion of MOA importance as INPs holds at other temperatures.

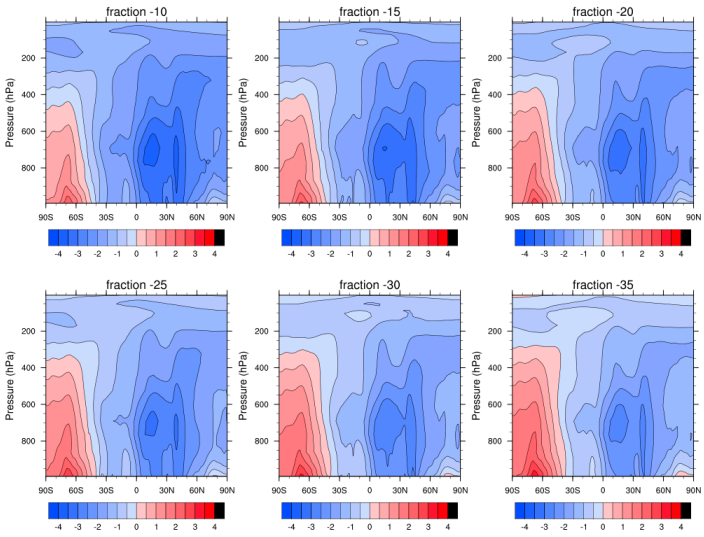

Figure R3. Vertical cross sections of ratio of MOA INP concentration to dust INP concentration. INP concentrations are diagnosed at different temperatures (from –10 to –35°C).

To improve the clarity of Figures 4 and 5, we have added a sentence in the figure caption as follows:

"Simulated INPs data are sampled at the same pressures, longitudes and latitudes as the field measurements."

Line 552-561: I generally agree with the explanation for the observed differences shown in Fig.6d. However, how does the model handle the sea ice coverage over the Southern Ocean during Austral winter? As the sea ice extent should extend as far north as approximately 60 S. Therefore, it important to know how the model handles the emission of MOA during the austral winter and spring months, especially as the sea ice extent is prescribed based on climatology (see lines 354-356). Does this mean that the entire year assumes a constant sea ice extent or does it change based on season. Depending on how this is handled, it could have large implications for both the INP and CCN distribution due to MOA emissions.

We thank reviewer for the great suggestion. See our reply to your general comment. In CESM2-CAM6, the prescribed sea ice extent changes with season, and each month is different.

Figure 7: How does the model produce ice nucleation or even MOA at such high latitudes in the Southern Hemisphere at the surface when the center of the Antarctic ice sheet is ~3000 m (700 hPa)?

We thank the reviewer for the comment. We agree with the reviewer that the mountains and ice sheets in the Antarctic are around 3 km in height, and our model also did not have data over these regions. However, there are still some regions at high latitudes in the Southern Hemisphere, where the surface heights are below 400 m at 80° S south (see Figure R3 below). Considering Figure 7 is the annual zonal mean, which includes the data from the summer season and low surface height regions, the data can be extended to low altitudes at high latitudes. We also note that surface level values are very small in Fig.7a.

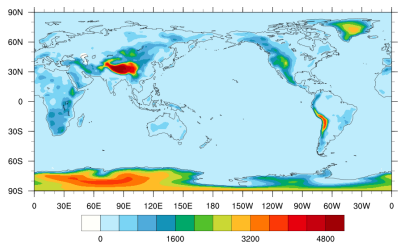

Figure R4. Global surface height.

Line 579-581: Mentioning seasonal dependence is quite interesting especially concerning my previous comment about the sea-ice extent. Therefore, I think it would be worthwhile to show how the emission of MOA changes over the Southern Ocean between austral summer and winter and how this influences the freezing rates.

That is a very good question, and we added some plots here. We notice that the MOA nucleation rate is strongly dependent on the MOA mass mixing ratio in mixed-phase clouds. The mass mixing ratio of MOA in mixed-phase cloud regions is related to the MOA emission, general circulation (transport), and wet removal (by precipitation). Even though MOA has a smaller emission rate during the austral winter, the effective transport and ice nucleation enhances the ice nucleation rate of MOA in the mixed-phase clouds.

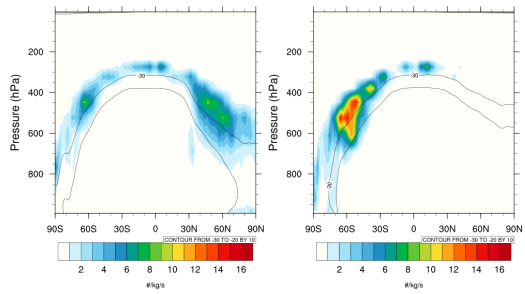

Figure R5. Latitude-pressure cross-sections of annual mean MOA ice nucleation rate in the austral summer (left) and winter (right).

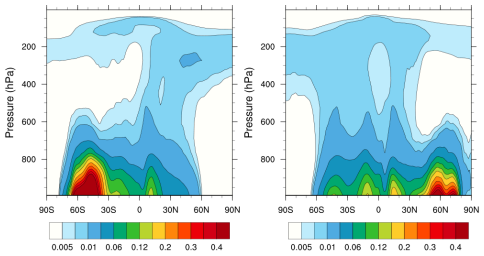

Figure R6. Latitude-pressure cross-section in the austral summer (left) and winter (right).

Line 590-592: What does this increase in percent mean? Can you report the change in the number of CDNUMC? Also the fact that there is a difference between austral summer and winter might point to a change in the sea ice extent in the model as well as biological activity.

We thank the reviewer for the suggestion. To increase the clarity, we revised the sentence in section 3.4 to report the change in the number of CDNUMC and also point to a change in the sea ice extent as

"The vertically-integrated cloud droplet number concentration (CDNUMC) increases by 7.5×10^4 cm^{-2} (5.25% in percent change) on the global annual mean, and by 1.1×10^4 cm^{-2} (0.94%) and 3.2×10^5 cm^{-2} (16.89%) over 20–90°S during the austral winter (June-July-August) and summer (December-January-February), respectively, by comparing B14_D15_M18 with CTL. This reflects a strong seasonal variation of MOA emissions due to changes in the sea ice extent as well as biological activity."

Line 599: why do you switch to an isotherm of -15 now? Previously the -25 isotherm was used and the figures also have the -20 isotherm. Perhaps it is better to be consistent and choose one isotherm throughout or at least explain why different isotherms are chosen.

We thank the reviewer for the comment. We selected the –25°C isotherm level in Figure 6 for a consistent comparison with previous studies (e.g., McCluskey et al., 2019). The –15°C isotherm level was selected in Figure 8 to better represent the mixed-phase cloud feature. –15°C is the most effective temperature for the WBF process, and at this temperature the mixed-phase cloud properties show larger changes than –25°C after introducing more INPs.

We have revised the caption of Figure 8 as follows to explain why we choose another isotherm:

"Figure 8. Annual zonal-mean distributions of (a) surface CCN concentration at S=0.1%, (b) cloud ice number concentration on T=–15°C isotherm, (c) vertically-integrated cloud droplet number concentration, (d) cloud ice mass mixing ratio on T= –15°C isotherm, (e) liquid water path over ocean, (f) ice water path, (g) shortwave cloud forcing, and (h) longwave cloud forcing for CTL (black), B14_D15 (orange), and B14_D15_M18 (green), along with available observations (gray dashed lines) as references. The -15°C isotherm level was used in (b) and (d) to show stronger changes in the mixed-phase cloud properties than the -25°C isotherm."

Line 628-630: Could this also be due to sea ice extent?

We thank the reviewer for the suggestion. We agree with the reviewer and revised the sentence as

"We also notice that CCN, CDNUMC, and SWCF show smaller changes during the austral winter due to weaker oceanic biological activity and larger sea ice extent."

Line 655-661: Discussion on the differences between bubble bursting (which is implemented in the model) and jet drops (which is not) does not seem necessary. Perhaps it is just fine to just mention that more observations/ fundamental understanding are needed for implementation of jet drops as is not clear why the differences in size of the emitted aerosols matter here. If this is important, please expand on why that could make a significant difference to the observed results and overall importance of MOA.

We thank the reviewer for the suggestion. We explained why jet drops could be potentially important by adding to the discussion:

"These large aerosol particles from jet drops are more effective as CCN and INPs."

Editorial comments:

Line 47: "replace to" with "and" as the sentence should read: "temperature is between -38 and 0..."

Done. Thanks.

Line 49: Please consider rephrasing the sentence to read: "INPs have different characteristics depending on their composition and origin" as it does not make sense as it is written.

Thanks. We have revised the sentence to read as

"INPs have different characteristics depending on their composition and origin."

Line 52: Consider adding some citations when you mention the uncertainty in the ability of black carbon to act as INPs. To my understanding, the evidence is mounting that BC is irrelevant in the MPC region.

Thanks. We agree with the reviewer that there is mounting evidence that BC is irrelevant in the mixed-phase cloud regime (Adams et al., 2020; Kanji et al., 2020; Schill et al., 2020). So we removed this sentence in the revised manuscript:

"However, large uncertainties exist surrounding the ice nucleating properties of black carbon and organic carbon from biomass burning and fossil fuel combustion."

Line 74: Please add Ault et al, 2013 to the reference list.

Thanks. We have added Ault et al., 2013 to the reference list.

Line 123: Please add "method" or something similar after: "[Chl-a]-based"

Thanks. We added "method" after "[Chl-a]-based".

Figure 1: Fix unit for micro

Thanks. We have fixed the unit in Figure 1.

Figure 3: The 0.1 % supersaturation is not showing up well. Also, the longitude representation (248 W) seems a bit odd, but perhaps that's just a personal preference. In the Figure caption, it might be nice to state that percent change in surface CCN comes from comparing B14-BASE.

We thank the reviewer for the suggestion. We have fixed the issues with Figure 3. We revised the figure caption of Figure 3 as following:

"Figure 3. Spatial distribution of annual mean percentage changes of surface CCN concentrations at 0.1% supersaturation due to MOA (by comparing B14_D15 and BASE), and vertical distribution of CCN concentrations at 0.1% supersaturation from eight measurements (solid gray lines), BASE (solid orange line) and B14_D15 (solid green line)..."

Figure 4: Consider flipping the color bar so that the warmest temperatures are at the top and the coldest at the bottom.

Thanks. We have changed the color bar as suggested.

Figure 6: Please fix panel d to be consistent with the other panels.

Thanks. We have fixed d. We also note that panel d is a different type of figure from other panels but we think it is better to put it together with other panels in Figure 6 than itself stand-along as a separate figure. The revised Figure 6 looks

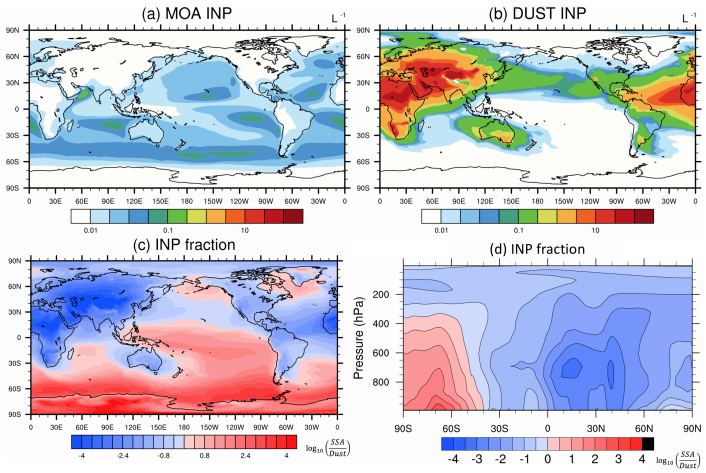

References

Adams, M. P., Tarn, M. D., Sanchez‐Marroquin, A., Porter, G. C. E., O'Sullivan, D., Harrison, A. D., et al. (2020). A major combustion aerosol event had a negligible impact on the atmospheric ice‐nucleating particle population. Journal of Geophysical Research: Atmospheres, 125, e2020JD032938. https://doi.org/10.1029/2020JD032938

DeMott, P. J., Prenni, A. J., Liu, X., Kreidenweis, S. M., Petters, M. D., Twohy, C. H., Richardson, M. S., Eidhammer, T. and Rogers, D. C.: Predicting global atmospheric ice nuclei distributions and their impacts on climate, Proceedings of the National Academy of Sciences of the United States of America, 107(25), 11217–11222, doi:10.1073/pnas.0910818107, 2010.

DeMott, P. J., Prenni, A. J., McMeeking, G. R., Sullivan, R. C., Petters, M. D., Tobo, Y., Niemand, M., Möhler, O., Snider, J. R., Wang, Z. and Kreidenweis, S. M.: Integrating laboratory and field data to quantify the immersion freezing ice nucleation activity of mineral dust particles, Atmospheric Chemistry and Physics, 15(1), 393–409, doi:10.5194/acp-15-393-2015, 2015.

Kanji, Z. A., Welti, A., Corbin, J. C., & Mensah, A. A. (2020). Black carbon particles do not matter for immersion mode ice nucleation. Geophysical Research Letters, 46, e2019GL086764. https://doi.org/10.1029/2019GL086764

McCluskey, C. S., Ovadnevaite, J., Rinaldi, M., Atkinson, J., Belosi, F., Ceburnis, D., Marullo, S., Hill, T. C. J., Lohmann, U., Kanji, Z. A., O'Dowd, C., Kreidenweis, S. M. and DeMott, P. J.: Marine and Terrestrial Organic Ice-Nucleating Particles in Pristine Marine to Continentally Influenced Northeast Atlantic Air Masses, Journal of Geophysical Research-Atmospheres, 123(11), 6196–6212, 2018a.

McCluskey, C. S., Hill, T. C. J., Humphries, R. S., Rauker, A. M., Moreau, S., Strutton, P. G., Chambers, S. D., Williams, A. G., McRobert, I., Ward, J., Keywood, M. D., Harnwell, J., Ponsonby, W., Loh, Z. M., Krummel, P. B., Protat, A., Kreidenweis, S. M. and DeMott, P. J.: Observations of Ice Nucleating Particles Over Southern Ocean Waters, Geophysical Research Letters, 45(21), 11,989-11,997, doi:10.1029/2018GL079981, 2018b.

McCluskey, C. S., DeMott, P. J., Ma, P. L. and Burrows, S. M.: Numerical Representations of Marine Ice-Nucleating Particles in Remote Marine Environments Evaluated Against Observations, Geophysical Research Letters, 46(13), 7838–7847, doi:10.1029/2018gl081861, 2019.

Schill, G. P., DeMott, P. J., Emerson, E. W., Rauker, A. M. C., Kodros, J. K., Suski, K. J., Hill, T. C. J., Levin, E. J. T., Pierce, J. R., Farmer, D. K. and Kreidenweis, S. M.: The contribution of black carbon to global ice nucleating particle concentrations relevant to mixed-phase clouds, Proceedings of the National Academy of Sciences of the United States of America, 117(37), 22705–22711, doi:10.1073/pnas.2001674117, 2020.

Shi, Y., and Liu, X.: Dust Radiative Effects on Climate by Glaciating Mixed-Phase Clouds, Geophys Res Lett, 46, 6128-6137, 10.1029/2019GL082504, 2019.

Vergara-Temprado, J., Holden, M. A., Orton, T. R., O'Sullivan, D., Umo, N. S., Browse, J., Reddington, C., Baeza-Romero, M. T., Jones, J. M., Lea-Langton, A., Williams, A., Carslaw, K. S. and Murray, B. J.: Is Black Carbon an Unimportant Ice-Nucleating Particle in Mixed-Phase Clouds?, Journal of Geophysical Research: Atmospheres, 123(8), 4273–4283, doi:10.1002/2017JD027831, 2018.

727

728

Effects of Marine Organic Aerosols as Sources of Immersion-Mode Ice Nucleating Particles on High Latitude Mixed-Phase Clouds

Xi Zhao[1], Xiaohong Liu[1], Susannah Burrows[2], and Yang Shi[1],

[1]Department of Atmospheric Sciences, Texas A&M University, College Station, Texas, 77840, USA
[2]Pacific Northwest National Laboratory, Richland, Washington, 99352, USA

Correspondence to: Xiaohong Liu (xiaohong.liu@tamu.edu)

Abstract. Mixed-phase clouds are frequently observed in high latitude regions, and have important impacts on the surface energy budget and regional climate. Marine organic aerosol (MOA), a natural source of aerosol emitted over ~70% of Earth's surface, may significantly modify the properties and radiative forcing of mixed-phase clouds. However, the relative importance of MOA as a source of ice nucleating particles (INPs) in comparison to mineral dust, and its effects as cloud condensation nuclei (CCN) and INPs on mixed-phase clouds are still open questions. In this study, we implement MOA as a new aerosol species into the Community Atmosphere Model version 6 (CAM6), the atmosphere component of the Community Earth System Model version 2 (CESM2), and allow the treatments of aerosol-cloud interactions of MOA via droplet activation and ice nucleation. CAM6 reproduces observed seasonal cycles of marine organic matter at Mace Head and Amsterdam Island when the MOA fraction of sea spray aerosol in the model is assumed to depend on sea spray biology, but fails when this fraction is assumed to be constant. Model results indicate that marine INPs dominate primary ice nucleation below 400 hPa over the Southern Ocean and Arctic boundary layer, while dust INPs are more abundant elsewhere. By acting as CCN, MOA exerts a shortwave cloud forcing change of –2.78 W m^{-2} over the Southern Ocean in the austral summer. By acting as INPs, MOA enhances the longwave cloud forcing by 0.35 W m^{-2} over the Southern Ocean in the austral winter. The annual global mean net cloud forcing changes due to CCN and INPs of MOA are –0.35 and 0.016 W m^{-2}, respectively. These findings highlight the vital importance of Earth System Models to consider the MOA as an important aerosol species for the interactions of biogeochemistry, hydrological cycle, and climate change.

删除了： the

删除了： Arctic, Antarctic, and over the Southern Ocean

1 Introduction

Ice crystals in clouds play a critical role in determining cloud phase, lifetime, electrification, and radiative properties. As a result, cloud ice influences precipitation and cloud radiative forcing. To quantify the impact of ice crystals on the hydrologic cycle and energy budget of the Earth system, it is important to advance the process-based understanding of initiation and evolution of ice particles. Ice particles can be initialized by homogeneous freezing or by heterogeneous nucleation. Homogeneous freezing of cloud droplets and aerosol solution droplets happens when air temperature is below approximately –38° C. In mixed-phase clouds in which air temperature is between –38° C and 0° C, ice is initialized only by heterogeneous nucleation on ice nucleating particles (INPs) (Vali et al., 2015).

INPs have different characteristics depending on their composition and origin. Previous studies (Hoose and Möhler, 2012; Murray et al., 2012; Kanji et al., 2017) have shown that mineral dust, primary bioaerosols (e.g., fungal spores, bacteria, and pollen), and volcanic ash can be effective INPs. However, large uncertainties exist surrounding the ice nucleating properties of black carbon (Schill et al., 2020; Vergara-Temprado et al., 2018) and organic carbon from biomass burning and fossil fuel combustion. A majority of INPs are of terrestrial origin. Due to their large emission quantities and high efficiency at forming ice, mineral dust may play a dominant role in ice formation over continents. However, in remote oceanic regions where terrestrial INPs are rare, the aerosol species contributing to INPs and the mechanisms for ice initialization remain poorly understood. Recent observational and modelling studies have shown that marine organic aerosol (MOA) is potentially an important source of INPs over remote oceanic regions (Wilson et al., 2015; DeMott et al., 2016; Vergara-Temprado et al., 2017; Huang et al., 2018; McCluskey et al., 2019).

MOA can be generated from both primary and secondary processes during ocean biological activities, producing either water-soluble or insoluble organic aerosols. Previous studies have inferred that water-insoluble marine organic matter is mainly derived from the primary emissions of sea spray aerosols (SSAs) (Ceburnis et al., 2008). In this production process, SSAs and associated organic matter are injected into the marine boundary layer when bubbles burst at the air-sea interface. Long-term measurements of

删除了： to

删除了： Kanji

删除了： 2017

删除了： INPs have different characteristics in their compositions and origins. Previous studies

804 seasonal variability in SSAs (O'Dowd et al., 2004; Yoon et al., 2007; Rinaldi et al., 2013)
805 and organic matter in remote marine air (Sciare et al., 2009) are consistent with the
806 hypothesis that the amount of organic matter is associated with ocean biological activity.
807 Laboratory experiments have also demonstrated that the presence of phytoplankton blooms
808 can be associated with significant changes in the number flux and size distribution of
809 emitted SSAs (Ault et al., 2013, Alpert et al., 2015; Rastelli et al., 2017; Forestieri et al.,
810 2018; Christiansen et al., 2019), as well as the SSA organic content (Facchini et al., 2008;
811 Ault et al., 2013).
812 Parameterizations for the primary emission of MOA have been developed with the
813 intention to be used in models. Most of these parameterizations relate MOA emission flux
814 to ocean chlorophyll a concentration [Chl-a]. An advantage of this approach is that [Chl-a]
815 is globally available from satellite-based measurements, especially over the remote oceans
816 where ground-based observations are difficult to conduct. Although [Chl-a] makes up only
817 a minor fraction of the organic matter in the ocean (Gardner et al., 2006), it has a long
818 history as a widely-used proxy for the biomass of phytoplankton in ocean surface waters
819 (Steele et al., 1962; Cullen et al., 1982), and has been used to derive empirical relationships
820 between satellite-observed [Chl-a] and the observed MOA contribution to submicron SSAs.
821 Several studies have also found that measured organic matter in SSA correlates more
822 strongly with ocean [Chl-a] than with other satellite-retrieved ocean chemistry variables,
823 such as particulate organic carbon, dissolved organic carbon, and colored dissolved and
824 detrital organic matter (O'Dowd et al., 2004; Sciare et al., 2009; Gantt et al., 2011; Rinaldi
825 et al., 2013).
826 O'Dowd et al. (2008) proposed a MOA emission parameterization, which was further
827 modified by Langmann et al. (2008) and Vignati et al. (2010). In this parameterization, the
828 fraction of emitted organic matter in SSA has a linear relationship with ocean [Chl-a] and is
829 not dependent on surface wind speed. Gantt et al. (2011) took a step further, and developed
830 an emission parameterization in which the organic matter fraction is an empirical function
831 of ocean [Chl-a], 10 m wind speed, and aerosol size. Both parameterizations from Gantt et
832 al.(2011) and Vignati et al. (2010) were found to capture the magnitude of MOA
833 concentrations compared to observations, but the parameterization from Gantt et al. (2011)
834 had a better representation of seasonal variability of MOA concentrations at Amsterdam

Island and Mace Head, Ireland (Meskhidze et al., 2011). Rinaldi et al. (2013) also developed a MOA emission parameterization which depends on surface wind speed and [Chl-a], and by assuming an 8–10 day time lag between upwind ocean [Chl-a] and enhanced production of MOA the correlation between enriched MOA and [Chl-a] was improved. Burrows et al. (2014) proposed a physically-based approach to represent MOA emission process (i.e., OCEANFILMS) instead of using the empirical [Chl-a]. This method was implemented in the DOE Energy Exascale Earth System Model version 1 (E3SMv1) (Golaz et al., 2019; Rasch et al., 2019), and the CCN effect of MOA on cloud droplet activation was investigated (Burrows et al., 2018).

Recent observational evidence continuously shows the importance of MOA as INPs in natural clouds (Wilson et al., 2015; DeMott et al., 2016; McCluskey et al., 2018a, b). However, there have been very limited modeling studies to quantify the effects of MOA INPs on clouds. Yun and Penner (2013) conducted the first global study of MOA on ice formation and radiative forcing using the CAM3 model. Their study indicated that MOA INPs are the dominant INPs for mixed-phase clouds over the Southern Hemisphere (SH), and after including MOA INPs, the model generated a more reasonable ice water path (IWP) compared with the International Satellite Cloud Climatology Project (ISCCP) observation data. In their study, the model simulated frozen fraction of MOA at –15°C is 3.75% for their lowest size bin (0.05 – 0.63 μm) and 100% for their larger size bins. These values may be too high compared with both historical and recent measurements of the ice nucleation efficiency of sea surface material (Schnell and Vali, 1975; Wilson et al., 2015) and SSAs (DeMott et al., 2016; McCluskey et al., 2018b).

With more measurements of MOA and sea spray INPs becoming available, recent modeling studies have been able to improve upon past MOA INP parameterizations. Huang et al. (2018) used the ECHAM6-HAM2 model to study the MOA influence on ice formation and climate. They followed the [Chl-a]-based method of Rinaldi et al. (2013) to represent the MOA emission and compared two empirical methods for calculating the MOA INP efficiency (Wilson et al., 2015; DeMott et al., 2016). They found that MOA influenced the cloud ice number concentration and effective radius only slightly, and MOA did not exert a significant influence on the global radiative balance due to compensating

cloud responses. However, these conclusions also depend on the sensitivity of their model to the change in INP number concentration.

In contrast to the findings of Huang et al. (2018), Vergara-Temprado et al. (2017) and McCluskey et al. (2019) found that MOA was the dominant source of INPs over the Southern Ocean. Vergara-Temprado et al. (2017) used the Global Model of Aerosol Processes (GLOMAP) to investigate the relative importance of feldspar and MOA for ice nucleation. Ice nucleation by MOA follows the Wilson et al. (2015) parameterization. This study also found that on 10–30 % of days in the study period there were more MOA INPs than feldspar INPs over the Northern Hemisphere (NH) Ocean. McCluskey et al. (2019) used the aerosol concentrations calculated offline from the Community Atmosphere Model version 5 (CAM5) to show that MOA is the dominant INPs over the Southern Ocean. Ice nucleation by MOA follows the McCluskey et al. (2018b) parameterization.

Isolating the INP effect of MOA on clouds and radiative forcing has rarely been examined directly, which motivates our study to address MOA ice nucleation process and to better understand the climate influence of MOA INPs. Our approach is different from previous studies. For example, we use a more physically-based approach (Burrows et al., 2014) to represent MOA emission instead of the empirical [Chl-a] based method used in Huang et al. (2018). Instead of the offline evaluation of INP parameterizations in CAM5 (McCluskey et al., 2019), this study implements the MOA emission and other process representations in the Community Atmosphere Model version 6 (CAM6), the latest atmosphere component of Community Earth System Model version 2 (CESM2), and allows for the impacts of MOA on modeled clouds and radiative forcing interactively. Lastly, we isolate the INP effect from the CCN effect of MOA in order to better understand the MOA influence on clouds via these two mechanisms.

This paper is organized as follows. Section 2 presents the model, parameterizations of MOA as well as model experiments. Section 3 describes the model results and comparison with observations. Section 4 discusses the remaining questions. Section 5 summarizes and draws the conclusions of this study.

2 Methods

2.1 Model and parameterizations

CAM6 with the Finite-Volume (FV) dynamical core (Lin and Rood, 1997) is used in this study. CAM6 treats important physical processes in the atmosphere, including radiative transfer, deep convection, cloud macrophysics, cloud microphysics, shallow convection, and planetary boundary layer turbulence. Cloud and aerosol interactions with longwave and shortwave radiation transfer are treated by the Rapid Radiative Transfer Model for GCMs (RRTMG) scheme (Iacono et al., 2008; Mlawer et al., 1997). A double-moment scheme (Gettelman et al., 2015) is used to describe the microphysical processes of cloud and precipitation hydrometeors in large-scale stratiform clouds, while the deep convection is represented by the Zhang and McFarlane (1995) scheme. CAM6 uses the Cloud Layers Unified By Binormals (CLUBB) scheme (Golaz et al., 2002; Larson et al., 2002) to unify the representations of cloud macrophysics, turbulence, and shallow convection.

The four-mode version of the Modal Aerosol Module (MAM4), which is an extension of the three-mode version of MAM (Liu et al., 2012), is used to describe the aerosol properties and processes in CAM6 (Liu et al., 2016). MAM4 uses the modal method to represent the size distributions of four aerosol modes: Aitken, accumulation, coarse, and primary carbon. The original MAM4 encompasses six aerosol species: black carbon, dust, primary organic aerosol, sea salt, secondary organic aerosol, and sulfate (Table 1). The primary organic aerosol here refers to non-marine sources of organic matter, usually from terrestrial biomass burning, fossil fuel, and biofuel burning. Aerosol species are internally-mixed within a mode and externally-mixed between modes. Then the log-normal size distribution can be determined for each mode based on a prescribed geometric standard deviation (Table 1). Different aerosol species are characterized by a variety of properties such as hygroscopicity, density, and optical properties (Table 2).

MAM in CAM6 adopts the modal approach, where aerosol species are assumed to be internally mixed within a mode, and externally mixed between modes. MOA is emitted into the fine aerosol modes with different assumptions of mixing state with inorganic sea salt: (1) MOA is emitted into the Aitken and accumulation modes together

删除了： The mass mixing ratio of each aerosol species within a mode and the total number mixing ratio of aerosols in that mode are predicted in the model. …

with sea salt in the case of internally mixed with sea salt; or (2) MOA is emitted into the Aitken and primary carbon mode separately from sea salt in the case of externally mixed with sea salt. In addition, there is another assumption of whether the experimentally derived parameterizations of SSA mass emission flux represent the total emission of MOA and sea salt or only account for the emission of sea salt. In the former case, MOA will *replace* the mass and number emission fluxes of sea salt. In the latter case, MOA will *add* onto the sea salt mass and number emission fluxes. Burrows et al. (2018) tested different combinations of the two assumptions and found that the "internally-mixed" and "added" MOA approach provides the most physically realistic configuration compared to the observations. Thus, in our study we use this configuration but acknowledge that current observations do not provide precise constrains on the mixing state.

While anthropogenic aerosol and precursor gas emissions are prescribed for model simulations, emissions of natural aerosols (e.g., SSA, dust) are calculated interactively in the model. SSA in MAM is emitted following the parameterization of Mårtensson et al. (2003) for dry particle diameters from 0.020 to 2.8 μm, and Monahan et al. (1986) from 2.8 to 10 μm. The Mårtensson et al. parameterization is derived from laboratory experiments in which particles were produced by bubble bursting using a sintered glass filter in synthetic seawater. The emission rate depends linearly on the sea surface temperature and is proportional to 10-m wind speed, raised to the power of 3.41 (Monahan et al., 1986; Gong et al., 1997).

2.2 MOA in CAM6

In this study, several modifications are implemented in CAM6 in order to explicitly quantify the influence of marine organic matter on aerosols, clouds, and radiation. These modifications are comprised of (1) emission schemes of MOA, as introduced in section 2.2.1, and (2) ice nucleation parameterizations for MOA, as introduced in section 2.2.2.

2.2.1 Emission of MOA

Three different methods for online MOA emissions are implemented in CAM6. These methods parameterize the organic mass fraction of sea spray and use the fraction to compute MOA emissions based on the emission rate of SSA.

The mass fraction of MOA in total SSA, $F_{MOA/SSA}$ is defined as the following:

$$F_{MOA/SSA} = \frac{M_{MOA}}{M_{sea\ spray}} = \frac{M_{MOA}}{M_{MOA}+M_{sea\ salt}} \quad (1)$$

in which M_{MOA} is the mass mixing ratio of MOA, and $M_{sea\ salt}$ is the mass mixing ratio of sea salt. Thus, the emitted MOA mass mixing ratio can be computed as:

$$M_{MOA} = \frac{F_{MOA/SSA} \times M_{sea\ salt}}{1-F_{MOA/SSA}} \quad (2)$$

The MOA number emission flux is calculated based on the MOA mass emission flux for a given particle diameter within the emission size range (from 0.020 to 2.8 μm for the Mårtensson et al. parameterization) and particle density of MOA, the latter of which is set to be 1601 kg m^{-3} (Liu et al., 2012), as given in Table 2.

删除了： The emitted MOA number mixing ratio is calculated based on the emitted mass mixing ratio and particle density of MOA, the latter of which is set to be 1601 kg m^{-3} (Liu et al., 2012), as given in Table 2.…

Differences between the three emission methods lie in how to determine the organic mass fraction $F_{MOA/SSA}$. These methods are compared in this study: the first is the Langmuir isotherm-based parameterization by Burrows et al. (2014) (B14), the second is based on wind speed and [Chl-a] by Gantt et al. (2011) (G11), and the third, which represents a null hypothesis, assumes a fixed mass fraction between organic matter and sea salt (NULL).

a. G11 emission scheme

A chlorophyll-based emission scheme of MOA was derived based on the [Chl-a] and the 10-m wind speed (Gantt et al. (2011), hereafter referred to as G11). In this method, the organic mass fraction of sea spray is parameterized as:

$$F_{MOA/SSA} = \frac{\frac{1}{1+0.03\times e^{6.81\times D_p}}+0.03}{1+e^{-2.63\times(Chl-a)+0.18U_{10}}} \quad (3)$$

where D_p is the dry diameter of particles.

b. B14 emission scheme

Different from the earlier empirical chlorophyll-based scheme, a physically-based scheme, named OCEANFILMS was proposed for modeling the relationship between emitted SSA chemistry and ocean biogeochemistry (Burrows et al. (2014), hereafter referred to as B14). The Langmuir isotherm-based mechanism is adopted to describe the organic enrichment on the bubble film. When the bubble film bursts, the film breaks up into film drops, which are suspended in the air. After evaporation of water from these droplets, the remaining suspending materials form MOA and sea salt aerosol particles. In this method, the organic matter on one side of the bubble film (per area) is determined by:

$$M_{s\_MOA} = S_m \times \theta \quad (4)$$

where S_m is the organic mass per area at saturation (Table 3), and θ is the surface coverage fraction of organics calculated based on the Langmuir adsorption equilibrium assumption:

$$\theta = \frac{\alpha \times C_M}{1+\alpha \times C_M} \quad (5)$$

where α is the Langmuir parameter as prescribed in Table 3, and C_M is the mass concentration of organic matters in the ocean. C_M is prescribed from the monthly mean surface distribution of macromolecule concentrations, which is generated by ocean biogeochemical simulations (Burrows et al., 2014). In this method, three different organic classes are considered with molecular weights and mass per area at saturation as prescribed in Table 3.

Based on Equations (1), (4), and (5), the organic mass fraction of sea spray is expressed as:

$$F_{MOA/SSA} = \frac{S_m \times \frac{\alpha \times C_M}{1+\alpha \times C_M}}{S_m \times \frac{\alpha \times C_M}{1+\alpha \times C_M} + M_{s\_sea\ salt}} \quad (6)$$

$M_{s\_sea\ salt}$ is the sea salt mass per area of bubble surface, which is set to be 0.0035875 g m^{-2}.

c. NULL emission hypothesis

Null hypothesis assumes that the organic mass fraction of SSA is constant, and does not vary geographically or seasonally. If we are to adopt a parameterization for the

seasonal dependence of MOA, it is desirable to demonstrate that the agreement with observations of MOA is improved by such a parameterization, compared with the null hypothesis that no such relationship exists. The choice of the "null" hypothesis is motivated in part by Quinn et al. (2014) and Bates et al. (2020), who measured roughly constant values of $F_{MOA/SSA}$ in SSAs generated at sea by using a floating device to generate and sample spray, during five sea-going ship campaigns. These studies measured $F_{MOA/SSA}$ values of roughly 0.7–0.9 in sub-0.180 μm particles, and roughly 0.05–0.3 in sub-1.1 μm particles.

Loosely following the results of Quinn et al. (2014) and Bates et al. (2020), we set $F_{MOA/SSA}$ to 0.8 in the Aitken mode, and to 0.05 in the accumulation mode (see Table 1 for the size ranges of Aitken and accumulation modes). For comparison, Facchini et al. (2008) measured SSA generated from oceanic water for its organic and salt content, and found that organic matter comprised roughly 75% of particles in the size range 0.125–0.250 μm, and that this fraction decreased with increasing particle size to about 5% of 1 μm particles. Similarly, Prather et al. (2013) analyzed sea spray generated in a wave tank during a mesocosm bloom experiment and reported that about 80% of 0.080 μm particles were classified as organic carbon by transmission electron microscopy (TEM) with energy-dispersive X-ray (EDX), while a few percents of 1 μm particles were classified as either organic carbon or biological species by the aerosol TOF mass spectrometry (ATOFMS).

2.2.2 Effects of MOA on clouds as CCN and INPs

MOA is emitted into different aerosol modes depending on mixing state of MOA and sea salt (Burrows et al., 2014, 2018). In the internally-mixed emission approach, MOA is emitted into the accumulation and Aitken modes along with sea salt, as shown in Table 1. In contrast, MOA is emitted into the Aitken and primary carbon modes in the externally-mixed emission approach. Furthermore, the emission of MOA can replace or be added to sea salt emission in terms of mass and number in the model. Burrows et al. (2018) found that simulated MOA amounts, seasonal cycles, and impacts on CCN over the Southern Ocean show better agreement with observations under the assumption that emitted MOA is added to, and internally mixed with sea salt. Thus, we used the

"internally-mixed" and "added" approach for MOA emission in this study. As shown in Table 2, the hygroscopicity of MOA is set to be 0.1 following Burrows et al. (2014, 2018), compared to 1.16 for sea salt. The mode hygroscopicity is calculated as the volume-weighted average of hygroscopicities of all species in a mode, which is then used in the Abdul-Razzak and Ghan (2000) droplet activation parameterization in CAM6. The mode hygroscopicity is reduced due to lower hygroscopicity of MOA. However, based on the method to calculate sea salt emission (Liu et al., 2012) for a given aerosol mode, the "added" MOA mass increases the number concentrations of particles in the Aitken and accumulation modes, which overcomes the reduction in mode hygroscopicity to activate more CCN.

In this study, in addition to the CCN effect of MOA, we also include its effect on clouds as INPs. For this purpose, two different ice nucleation parameterizations for MOA are implemented in CAM6. Additionally, we examine the relative importance of MOA to dust INPs with different ice nucleation parameterizations.

a. W15 ice nucleation scheme of MOA

An INP parameterization for MOA was proposed based on immersion-freezing measurements of materials aerosolized from sea surface microlayer (SML) water samples collected in the North Atlantic and Arctic Oceans (Wilson et al., 2015). In this parameterization (hereafter as W15), the number concentration of MOA INPs is a function of temperature (T) and the total organic carbon (TOC) mass concentration, given as:

$$N_{IN,T} = TOC \times e^{(11.2186-(0.4459\times T))} \quad (7)$$

In which, TOC is calculated as $M_{MOA} \times \frac{OC}{OM}$, where the $\frac{OC}{OM} = 0.5$ following McCluskey et al., 2018a.

W15 is developed based on the TOC in the sea surface microlayer samples, which may not be representative of ambient MOA. W15 assumes that relationship between TOC and INPs in airborne sea spray is the same as that in SML samples due to limited measurement data in the early stage. However, recent research suggests that INPs may be transferred differently from TOC during the sea spray production (Wang et al., 2017),

calling this assumption into question. The quantitative importance of this selective transfer of INPs from SML to the SSAs is a topic requiring further research beyond the scope of the current study and is not accounted for here. Additionally, this approach did not attempt to correct for the possible entrainment of multiple ice-nucleating entities into a single sea spray particle.

b. M18 ice nucleation scheme of MOA

Another empirical INP parameterization of MOA was derived based on the correlation between ambient aerosols and INPs measured during the "clean scenario" at Mace Head Station in August 2015 (McCluskey et al., 2018a, hereafter as M18). Therefore, M18 includes the effect of physiochemical selective emission and aerosol chemistry in the air which is missed in W15. This parameterization follows the same functional form as the surface-active site density (n_s) parameterization of Niemand et al. (2012) for dust, but with different coefficients for MOA, as given below:

$$n_s(T) = e^{(-0.545(T-273.15)+1.0125)} \quad (8)$$

MOA INP number concentration is then calculated by: $N_{INP}(T) = N_{tot} S_{ae} n_s(T)$, where S_{ae} and N_{tot} are the total surface area and number mixing ratio of SSA, calculated for the Aitken and accumulation modes, respectively.

c. N12 ice nucleation scheme of dust

A surface-active site density-based ice nucleation scheme for immersion freezing on dust was derived by Niemand et al. (2012) (hereafter referred to as N12) based on measurements of the AIDA cloud chamber. N12 relates the number concentration of dust INPs to the dust aerosol number concentration (N_{tot}), dust particle surface area (S_{ae}, calculated based on dry diameter of particles), and the density of ice-active surface sites ($n_s(T)$) at a given temperature T, shown as:

删除了： ($n_s(T)$)

$$N_{INP}(T) = N_{tot} S_{ae} n_s(T) \quad (9)$$

in which $n_s(T)$ is given as:

$$n_s(T) = e^{(-0.517(T-273.15)+8.934)} \quad (10)$$

N12 is valid in the temperature range from –36 to –12 ℃.

d. D15 ice nucleation scheme of dust

As the N12 scheme relates INPs to all sizes of dust aerosol, it may overestimate INPs, since smaller dust aerosol (<0.5 μm) may not be effective as INPs. An empirical ice nucleation scheme for the immersion freezing on dust aerosol with sizes larger than 0.5 μm was derived based on field and laboratory measurements (DeMott et al., 2015) (hereafter referred to as D15). The dust INP number concentration is calculated as

$$N_{INP}(T) = a(n_{0.5})^b e^{c(T-273.15)-d} \quad (11)$$

where a = 3, b = 1.25, c = –0.46, d =11.6, and $n_{0.5}$ is the number concentration of dust particles with diameters larger than 0.5 μm.

We note that the above ice nucleation parameterizations (W15, M18, N12, and D15) are based on empirical formulations. The default heterogeneous ice nucleation parameterization in CAM6 follows the classical nucleation theory (CNT) (Wang et al., 2014). CNT is a stochastic scheme that links the freezing rate to the number concentrations of dust and black carbon aerosols through different heterogeneous ice nucleation mechanisms (deposition, contact, and immersion). Due to large uncertainties in heterogeneous nucleation parameterizations, we conducted several ice nucleation sensitivity experiments in CAM6 as will be discussed in section 2.3.

2.3 Model configurations and experiments

In this study, we carried out several numerical experiments to investigate the influence of MOA on aerosols as well as CCN and INP activities (Table 4). All simulations were performed for 10 years with prescribed climatological sea surface temperatures and sea ice. The first year of simulations was treated as model spin-up, and last nine years of simulations were used in analyses. The simulations were driven by the present-day (year 2000) aerosol and precursor gas emissions with given greenhouse gas concentrations. The model was run for 32 vertical levels from surface up to 3 hPa with a horizontal resolution of 0.9° (latitudes) by 1.25° (longitude). We conducted two sets of

experiments. The first set of experiments, as listed in Table 4, are used to test the model sensitivity to different MOA emission schemes. The baseline experiment (BASE) uses the default CAM6 model which does not account for MOA emission and related physical processes. In addition to the BASE experiment, the B14 experiment addresses emission, advection, dry/wet deposition, and CCN effect of MOA using the Burrows et al. (2014) emission scheme. We also designed two additional experiments (G11 and NULL) to address the model sensitivity to emission methods. These simulations (B14 and G11) were conducted with the added and internally-mixed MOA approach, following Burrows et al. (2018). The INP effect of MOA is not considered in this set of experiments.

We conducted another set of experiments to investigate both CCN and INP effects of MOA, as listed in Table 4. The control experiment (CTL) is the same as BASE except that the D15 dust ice nucleation scheme was used to replace the CNT scheme in BASE, because D15 gave a better model performance compared with observations in our previous study (Shi and Liu, 2019). The B14_D15, which is based on CTL, considers the MOA emission from B14 and the CCN effect of MOA. The B14_D15_M18 experiment, which is based on B14_D15, additionally considers the INP effect of MOA based on M18. The comparison between CTL and B14_D15 shows the CCN effect of MOA, while the comparison between B14_D15 and B14_D15_M18 shows its INP effect.

We further conducted three experiments to examine the model sensitivity to a different MOA ice nucleation parameterization (i.e., W15) in B14_D15_W15, and to two different dust ice nucleation parameterizations (i.e., N12 and CNT) in B14_N12_M18 and B14_CNT_M18 by comparing them with the B14_D15_M18 experiment, respectively.

3 Results

3.1 Evaluation of modeled MOA

Given that a realistic representation of MOA emissions is a prerequisite for models to quantify its influence on ice nucleation, we evaluate three different MOA emission parameterizations in this section. We also analyze the processes contributing to MOA burden such as emission, transport, and removal, because the burden pattern

largely determines the INP distribution pattern. Comparisons with available observations are made to examine the performance of different MOA emission schemes.

Table 5 lists the annual global mean emissions and burdens of MOA and sea salt from different simulations. Overall, the G11 method generates the largest global MOA emission (27.1 Tg yr^{-1}) followed by the B14 method (24.5 Tg yr^{-1}). The magnitudes of MOA emissions are within the range of previous studies (Huang et al., 2018; Meskhidze et al., 2011; Langmann et al., 2008). The ratios of MOA emission to sea salt emission are 0.67% and 0.74% for the B14 and G11 experiments, respectively, which are also comparable to previous studies ranging from 0.3% to 3.2% (Huang et al., 2018; Meskhidze et al., 2011). The NULL approach only gives an annual global MOA emission of 4.6 Tg yr^{-1}, with the ratio of MOA emission to sea salt emission of 0.13%. These values are much lower than those of B14 and G11 approaches. We note that emissions and burdens of sea salt include the contribution from the coarse mode, which dominates the total sea salt emissions and burdens. We further evaluate aerosol mass mixing ratios and number concentrations in each aerosol mode in the B14 experiment, where MOA is added and internally mixed with sea salt. In B14, the ratio of MOA to sea salt mass burdens reaches up to 2.3 and 1.0 for the Aitken and accumulation modes, respectively. Number concentrations of accumulation mode aerosols near the surface are increased by up to 50% over some regions of the Southern Ocean and Arctic.

Despite the fact that there are differences in the global annual mean value, B14 and G11 generate similar spatial patterns of MOA emission rates (Fig. 1), while G11 tends to give higher emission rates than B14. Large emission rates are located in the mid-latitude storm tracks, equatorial upwelling, and coastal regions as shown in Fig. 1. These locations largely reflect the geographic distribution of primary ocean productivity as indicated by [Chl-a] (in G11) or organic matter concentrations (in B14).

Here we illustrate the influence of surface wind speeds (supplemental Fig. S1) on the emission of MOA. Although high MOA emissions are mostly co-located with vigorous oceanic biological activities, the oceanic area with smaller/larger wind speed tends to have a decreased/elevated emission rate relative to their biological activities. For instance, due to weak wind speeds (~5 m s^{-1}), a strong signal of oceanic organic matter concentration does not correspond to a large emission rate in the west coast of South

America. On the contrary, because of strong wind speeds (~10 m s^{-1}), moderate emission rates are noticed over the subtropical North Pacific Ocean and subtropical South Indian Ocean despite relatively small [Chl-a] or organic matter concentrations. This wind speed dependent pattern is more clearly shown in the B14 results than in the G11 results, because in the B14 emission scheme, $F_{MOA/SSA}$ is not related to the wind speed while SSA emission is proportional to the surface wind speed, as described in section 2.2.1. Conversely, $F_{MOA/SSA}$ is inversely related to the wind speed in G11, results in a more complicated relationship between wind speed and MOA emission rate in G11.

The global mean MOA burden is 0.097 Tg in B14, which is in close agreement with previous studies which suggested a range of 0.031 to 0.131 Tg (Huang et al., 2018; Burrows et al., 2018). The global distribution of MOA column burden shares the similar patterns between G11 and B14, with the peak burden around 1 mg m^{-2} over the mid-to high latitude Southern Ocean (Fig. 1). Despite the fact that large burdens are usually related to locations of high emissions, they are also influenced by advection (dependent on 3-D wind), dry deposition (dependent on particle size), and wet deposition (dependent on precipitation). The oceanic regions with small annual precipitation rates (supplemental Fig. S1) lead to considerable accumulations of MOA in G11 and B14. For instance, the peak burdens with maximum values of 0.4 to 0.6 mg m^{-2}, on either side of the Pacific tropical convection zone correspond to the subsidence induced dry zone (i.e., subsiding branch of Walker and Hadley circulations).

Zonally-averaged vertical distributions of MOA mass mixing ratio illustrate the vertical transport of MOA (Fig. 1). Simulations from G11 and B14 exhibit a maximum value of 0.35 μg kg^{-1} within the boundary layer, located in 40°–50°S of the Southern Ocean, while the maximum value is only 0.05 μg kg^{-1} in NULL. Globally, G11 shows slightly higher MOA mass mixing ratios over all latitudes compared with B14, and transports more MOA to high altitudes over the tropical regions. It is clear that MOA is accumulated in the lower troposphere, i.e. below 600 hPa in G11 and B14, and below 800 hPa in NULL. The reason is that MOA is generated over the oceans, especially over the storm track regions with high precipitation, limiting MOA mainly to the lower troposphere.

We further evaluate model simulated MOA concentrations with measurements at Mace Head (Ireland) and Amsterdam Island (Fig. 2). The B14 and G11 methods do well in capturing the observed seasonal variation of MOA concentrations at Amsterdam Island (Fig. 2a), although the model produces slightly higher MOA concentrations. At Mace Head, the two methods produce delayed concentration peaks by about one month compared with observations (Fig. 2b). The mass fraction of MOA in SSA (Fig. 2c) shows a better agreement between the model and observation. Both the simulated and observed organic mass fraction increase from March and reaches a peak in July, although the observed peak is broader. The sea ice extent prescribed in the model as a boundary condition has a strong seasonal variation over the Southern Ocean, as shown in supplementary Figure S2. This can greatly impact the emission of MOA there (e.g., low emission during the austral winter and early spring). The NULL approach does not reproduce observed seasonal cycles of MOA and significantly underestimates observed MOA concentrations due to the prescribed mass fraction (0.05) in the accumulation mode.

Based on our analyses and comparisons with observations, we show that B14 implementation of MOA emission into CAM6 reasonably captures the concentrations and seasonal variations of MOA. Next we will study the MOA effects on clouds via acting as CCN (section 3.2) and INPs (section 3.3), based on model experiments with the B14 emission (Table 4).

删除了： Next we will study the MOA effects on clouds with a focus on its INP effect, based on model experiments with the B14 emission (Table 4)…

3.2 Impact of MOA on CCN

After introducing MOA in the model, we notice an obvious increase in oceanic surface CCN concentrations at high latitudes. Figure 3 shows the spatial distribution of annual mean percentage changes in surface CCN concentrations at a supersaturation of 0.1% due to MOA, derived from the two experiments (CTL and B14_D15). From Fig. 3, the annual mean CCN concentration increases by 15%–35% over much of the oceans from 30°S to 70°S, with a maximum increase of 45% located over the Southern Ocean (60°S, 55°E). Other regions showing significant increases of CCN are over the pristine high latitudes, with increases of 25–35% from 60°S to Antarctica in the SH and from 60°N to 80°N in the NH. These results are comparable with previous results with an

average increase by 12% and up to 20% of CCN over the Southern Ocean (Meskhidze et al., 2011). Over low- and mid-latitude oceans, CCN changes due to MOA are smaller. Generally, the distribution of CCN change is consistent with the MOA emission pattern. The vertical profiles of CCN concentrations from the two model experiments and observations during the eight field campaigns are shown in Fig. 3. Clear increases of CCN concentrations in the boundary layer due to MOA are evident for campaigns over the ocean or coastal regions (SOCEX1, SOCEX2, ACE1, FIRE1, and ASTEX), with a maximum increase (26%) in ACE1. Observed CCN from FIRE1 shows a strong inversion of CCN below 800 hPa, and this inversion is challenging for the model due to its coarse vertical resolution. An obvious underestimation of CCN in the model is noticed at FIRE3 over the Arctic Ocean in Spring, which is attributed to the underestimated transport of air pollution caused by too strong wet scavenging in the model (Liu et al., 2012).

3.3 Impact of MOA on INPs

In order to examine the importance of MOA INPs, we compare modeled INPs from MOA versus dust as well as compare them with observations from several field campaigns in high latitudes (Fig. 4). Modeled INP concentrations from MOA are calculated online using M18 and W15 parameterizations (from B14_D15_M18 and B14_D15_W15 experiments, respectively), while dust INP concentrations are calculated online using D15, CNT, and N12 parameterizations (from B14_D15_M18, B14_CNT_M18, and B14_N12_M18 experiments, respectively). Modeled INP concentrations are computed based on aerosol concentrations at different temperatures and are selected at the same altitudes and locations as the observations. The measured INP data were obtained from Mace Head, the CAPRICORN campaign (Clouds, Aerosols, Precipitation, Radiation, and Atmospheric Composition over the Southern Ocean), Oliktok Point, Zeppelin, and the SOCRATES campaign (Southern Ocean Clouds, Radiation, Aerosol Transport Experimental Study) (McCluskey et al., 2018a; McCluskey et al., 2018b; Creamean et al., 2018; Tobo et al., 2019).

As illustrated in Fig. 4, the M18 parameterization tends to underestimate observed INP concentrations except at temperatures colder than –25℃. On the other hand, the W15

parameterization overestimates observed INP concentrations except at temperatures warmer than –20°C. Under the same MOA scenario, the W15 parameterization is more efficient in producing INPs than M18. This is because the M18 parameterization was derived from MOA in the atmosphere which accounts for the effect of physiochemical selective emission and aerosol chemistry in the air. In contrast, the W15 parameterization was derived based on the total organic carbon in sea surface microlayer samples, which contain higher organic mass concentrations compared with ambient MOA.

The dust INP concentration calculated with CNT shows an underestimation when temperature is warmer than –20°C and an overestimation when temperature is between –30°C and –20°C. This is consistent with previous work by Wang et al. (2014). The D15 parameterization indicates a clear underestimation. The N12 scheme has the better performance than D15 in Figure 4. However, the field campaigns used in Figure 4 are marine aerosol dominant/contained scenario campaigns. MOA is identified as an important INP source during these campaigns from measurements (McCluskey, Ovadnevaite, Rinaldi, et al., 2018b; McCluskey, Hill, Humphries, et al., 2018a). Thus, dust should not be expected to be the dominant INPs as indicated by the N12 scheme which only considers dust INPs. This suggests that N12 may overestimate dust INPs, which is consistent with our earlier study (Shi and Liu, 2019). These results suggest that the N12 parameterization is more efficient in producing dust INPs than the D15 parameterization under the same dust loading. INP concentrations from N12 are calculated based on the coarse, accumulation, and Aitken mode dust aerosol, which account for fine dust particles, while INP concentrations from D15 are calculated based on the number concentration of dust particles with diameters larger than 0.5 μm (DeMott et al., 2015). Simulated total INPs, the sum of dust and MOA INPs from D15 and M18, gives a better agreement with observations than D15 and M18 alone, although underestimations still exist at warmer temperatures.

Fig. 5 shows the comparison between simulated and measured INPs from five parameterization schemes as a function of temperature for the same field campaigns as in Fig. 4. Generally, an inverse linear relationship is revealed between $\log_{10}$(INPs) and temperature in the measurements. This relationship is also shown in simulated INP number concentrations from the empirical parameterizations (N12, D15, W15, M18). However, for

CNT, nearly constant INP number concentrations are presented at temperatures from –35℃ to –20℃, and then a rapid decrease with increasing temperature when temperature is warmer than –20℃. At temperatures higher than –15℃, nearly no INPs are produced by CNT, leading to the underestimation of INPs in the CNT method at these temperatures.

We notice higher INP number concentrations are produced from M18 compared with W15 at Zeppelin during March 2017. The most distinctive feature of this campaign is its very low aerosol loadings. For example, simulated SSA mass mixing ratio is around 0.6 μg kg^{-1} with the maximum value at 1.8 μg kg^{-1} below 850 hPa, and the dust mass mixing ratio is around 0.3 μg kg^{-1}. We note that simulated dust INP number concentrations from N12 are always higher than those from D15, and both N12 and D15 are more efficient in producing INPs than CNT when temperature is warmer than –20℃.

The global distribution pattern of annual mean MOA INP concentrations at 950 hPa at temperature of –25℃ is similar to that of MOA column burden concentrations, as shown in Fig. 6a. The MOA INPs are spread over the oceans, with peaks (~0.1 L^{-1}) over 40°S to 60°S of the Southern Ocean, the subtropical Southern Indian Ocean, the subtropical Atlantic Ocean, and the subtropical Eastern Pacific Ocean. Meanwhile, dust INP concentrations diagnosed at the same pressure and at the same temperature (Fig. 6b) are dominant over the NH and downwind of dust source regions in the SH (e.g., around Australia and extended to 50°S).

Fig. 6c shows the horizontal distribution of ratio of MOA INP concentration to dust INP concentration at 950 hPa. It is clear that MOA INPs are more important than dust INPs in the 40°S south of SH, where MOA INP concentrations can reach up to 1000 times higher than those of dust INPs. The zonal mean vertical distribution of ratio of MOA INP concentration to dust INP concentration is illustrated in Fig. 6d. The ratio peaks near 65°S, indicating that MOA INPs are more important than dust INPs over the Southern Ocean from surface up to 400 hPa, and extends poleward to 90°S. Above the 400 hPa altitude, dust particles are still more important INPs. Because dust particles are emitted over drier deserts (i.e., with lower precipitation and thus less wet scavenging), dust can be subject to long-range transport at high elevations. In contrast, most MOA particles are generated over the storm track regions with high occurrences of precipitation. Taking into account of emission, transport and wet scavenging of MOA and dust particles

results in MOA INPs dominating below 400 hPa over the Southern Ocean while dust INPs are generally more important elsewhere.

Immersion freezing on MOA in mixed-phase clouds requires that there are cloud droplets at temperatures colder than –4℃. Ice nucleation consumes cloud liquid water, and thus will compete with other processes for cloud liquid water (e.g., autoconversion of cloud water to rain, accretion of cloud water by rain and snow). This competition is expected to result in a reduction of ice nucleation rate of MOA compared with the offline calculation of ice nucleation rate as in McCluskey et al. (2019). Fig. 7 shows the annual zonal mean ice production rates from the immersion freezing of MOA and dust, which are calculated online for the cloud ice production tendency in the B14_D15_M18 experiment. Over the NH, the immersion freezing of dust dominates the primary ice production, giving an averaged ice production rate at 5 $kg^{-1}s^{-1}$ and up to 20 $kg^{-1}s^{-1}$ over 40°N at 400 hPa (Fig. 7b), while the MOA ice production rate is around 1 $kg^{-1}s^{-1}$ (Fig. 7a). However, in the Arctic boundary layer, the MOA fraction of total ice production rate is around 0.6~0.7 (Fig. 7c), indicating that MOA INPs are more important in generating ice crystals than dust INPs there. Over the SH, the immersion freezing rate of MOA dominates the primary ice production below 400 hPa with the MOA fraction close to 1. The zonal average ice nucleation rate of MOA is around 1 $kg^{-1}s^{-1}$, and up to 5 $kg^{-1}s^{-1}$ over the 65°S Southern Ocean at 400–600 hPa. The immersion freezing rate of dust is around 1 $kg^{-1}s^{-1}$ above 500 hPa, and smaller than 0.1 $kg^{-1}s^{-1}$ below 600 hPa altitude in the SH. Analysis of the seasonal variation of ice nucleation rate of MOA indicates that a maximum rate of about 16 $kg^{-1}s^{-1}$ occurs at 400–600 hPa over 60°S in July (austral winter). In summary, the annual mean immersion freezing of MOA dominates the primary ice production over the SH below 400 hPa altitude and in the Arctic boundary layer.

3.4 Impact of MOA on clouds and radiative forcing

Table 6 displays the differences of cloud and precipitation variables between the CTL and B14_D15_M18 experiments. With added MOA aerosol, the global annual mean surface concentration of CCN at 0.1% supersaturation changes from 103.3 cm^{-3} in CTL to 106.6 cm^{-3} in B14_D15_M18. This increase of 3.28 cm^{-3} is comparable to other model estimates of 3.66 cm^{-3} (Burrows et al., 2018), and 2.6–3.0 cm^{-3} (Meskhidze et al., 2011).

The vertically-integrated cloud droplet number concentration (CDNUMC) increases by 7.5×104 cm^{-2} (5.25% in percent change) on the global annual mean, and by 1.1×104 cm^{-2} (0.94%) and 3.2×105 cm^{-2} (16.89%) over 20–90°S during the austral winter (June-July-August) and summer (December-January-February), respectively, by comparing B14_D15_M18 with CTL. This reflects a strong seasonal variation of MOA emissions due to changes in the sea ice extent as well as biological activity. The global annual mean liquid water path (LWP), ice water path (IWP), longwave cloud forcing (LWCF), and total cloud fraction (CLDTOT) do not show obvious changes between CTL and B14_D15_M18. The global annual mean shortwave cloud forcing is stronger by –0.41 W m^{-2} due to MOA. During the austral summer over 20–90°S, we notice an increase of 4.57 g m^{-2} (5.10%) in LWP, and a 1.35% (2.52%) increase in low-cloud fraction. As a consequence, SWCF is enhanced by –2.87 W m^{-2} (Table 6), which is comparable to –3.5 W m^{-2} estimated in Burrows et al. (2018). Ice number concentration on –15ºC isotherm increases by 9.34% during the austral winter. There does not appear to be a significant change in LWCF, which is consistent with the result of Huang et al. (2018).

删除了： The vertically-integrated cloud droplet number concentration (CDNUMC) increases by 5.25% in B14_D15_M18 compared with CTL, and by up to 16.89% over 20–90°S during the austral summer (December-January-February)…

Strong CCN effect of MOA on clouds (in terms of significant changes in CCN and CDNUMC) tends to occur only in the SH over 40–60ºS, while strong INP effect (in terms of significant changes in cloud ice mass and number concentrations) is notable over 50–70º in both Hemispheres (Fig. 8). Over 40–60°S, a significant increase from 70 to 90 cm^{-3} in the annual zonal mean surface CCN concentration is observed. The CCN concentration there is nearly 30% higher in B14_D15 and B14_D15_M18 than in CTL. As a result, CDNUMC increases from 2.6×10^{10} m^{-2} in CTL to 3.0×10^{10} m^{-2} in B14_D15 and B14_D15_M18 over 40–60°S, leading to an increase in LWP due to the aerosol indirect effect (Fig. 8). Furthermore, we notice a stronger SWCF at 40–60°S by 3 W m^{-2} in B14_D15 compared with CTL. After considering the INP effect of MOA in the model, we notice that cloud ice number concentration and cloud ice mass mixing ratio increase in mixed-phase clouds which led to a slightly decrease in CDNUMC. As indicated in Fig. 8b,d, cloud ice number concentration increases from 4500 kg^{-1} in B14_D15 to 5500 kg^{-1} in B14_D15_M18 at ~60ºS, with cloud ice mass mixing ratio increased by 0.25 mg kg^{-1}. Over 60ºN, cloud ice number concentration increases from 4200 kg^{-1} in B14_D15 to 5200 kg^{-1} in B14_D15_M18, with cloud ice mass mixing ratio increased by 0.1 mg kg^{-1}.

Fig. 9 shows the seasonal variations of cloud properties and cloud radiative forcing averaged over the 20°S–90°S in SH, in response to the introduction of MOA as CCN and INPs. The seasonal variation of surface CCN concentration at 0.1% supersaturation shows the maximum value of 72 cm^{-3} in the austral summer and the minimum value of ~50 cm^{-3} in the austral winter in CTL. Similar seasonal variation patterns are also noted for CDNUMC and LWP. With the inclusion of MOA in the model, B14_D15 and B14_D15_M18 produce more surface CCN, with an increase of up to 14 cm^{-3} (~20%) in January, compared with CTL. Accordingly, CDNUMC increases from 2.1×10^{10} m^{-2} in CTL to 2.5×10^{10} m^{-2} in B14_D15 in January, and LWP increases from 93 g m^{-2} in CTL to 97 g m^{-2} in B14_D15 in January. As a consequence, SWCF is stronger by –3.5 W m^{-2} in B14_D15 compared with CTL during the austral summer. We also notice that CCN, CDNUMC, and SWCF show smaller changes during the austral winter due to weaker oceanic biological activity and larger sea ice extent.

Different from the warm cloud features above, seasonal variations of ice properties in mixed-phase clouds (i.e., cloud ice mass mixing ratio and number concentration on –15°C isotherm, IWP) clearly show winter maxima. After introducing the INP effect of MOA in the model, ice number concentration on –15°C isotherm increases by comparing B14_D15 with B14_D15_M18, with obvious increases of up to 27% in June. Ice mass mixing ratio on –15°C isotherm increases by 0.19 mg kg^{-1} (13%) in June. Increases in both cloud ice number and mass contribute to the increase of IWP by 0.5 g m^{-2} in austral winter. The seasonal change of LWCF is not well correlated with changes in ice number concentration and mass mixing ratio in mixed-phase clouds, because LWCF is controlled more by high clouds. Our introduction of MOA INPs mainly occurs in mixed–phased clouds, and therefore has a small influence on LWCF.

As shown in Table 7, the CCN effect of MOA on SWCF is strongest in the austral summer, with the value of –2.78 W m^{-2} over the 20°S–90°S in SH. In contrast, the INP effect of MOA on LWCF is strongest in the austral winter, with the value of 0.35 W m^{-2} (Table 8). For the net cloud forcing (SWCF + LWCF), the CCN effect of MOA is 2.65 W m^{-2} in the austral summer, and the INP effect is 0.65 W m^{-2} in austral spring over the 20°S–90°S. The annual global mean CCN and INP effects of MOA on the net cloud forcing are –0.35 and 0.016 W m^{-2}, respectively. From an annual mean perspective, the

CCN effect of MOA on SWCF is –0.84 W m^{-2} over 20–90°S and is about twice as much as the global mean value (–0.41 W m^{-2}), which indicates that the global annual mean SWCF change due to MOA is dominated by SH contributions.

4 Discussion

In this study, for the MOA emission process, we only considered the generation of MOA during the film drop breakup in B14, and the generation of MOA from jet drops is not currently included. The film drops form from bubble-cap films bursting, while the jet drops generate from the base of breaking bubbles. Particles from jet drops, with the diameter is around supermicrometer, are considered larger than particles from film drops (Wang et al., 2017). These large aerosol particles from jet drops are more effective as CCN and INPs. Extending the current emission scheme to include MOA emissions through jet drops (Wang et al., 2017) may be possible with more measurements and an improved understanding of physical mechanisms that determine the sea spray organic emission.

删除了： CCN or

删除了：

删除了： particles

For the ice nucleation efficiency of MOA, the M18 parameterization only includes the more persistent, heat-stable component observed in ambient sea spray aerosol INP sampling. This neglects the heat-labile organic INPs (McCluskey et al., 2018b). Regarding ice nucleation mechanisms, only the immersion mode of ice nucleation is implemented in this study, however, recent laboratory experiments (Wolf et al., 2019) have indicated a potentially important role of MOA in the deposition mode at temperatures below –40°C. Future work will focus on improving the limitations of the current understanding of MOA emission and ice nucleation in the model.

In this study, other potential INP species than dust and MOA, such as ash, biomass-burning particles, or other land-borne biological particles (Hoose et al., 2010; Jahn et al., 2020; Schill et al., 2020) are not represented in the model. These INP species can be regionally important at certain temperature regimes of mixed-phase clouds. Accounting for these species may increase the INP concentrations predicted in the model and change the mixed-phase cloud properties, particularly at warmer temperatures > -15°C. The impacts of these INP species will be quantified in our future studies.

Recent studies indicated an underestimation of ice formation in CAM6 (D'Alessandro et al., 2019) that results in too much cloud liquid and too little cloud ice in mixed-phase clouds. In addition to ice nucleation undertaken in this study, other factors may contribute to this model bias. For example, the CLUBB scheme used in CAM6 for turbulence and shallow convection treats only liquid phase condensation, lacking ice formation in the model's large-scale cloud macrophysics (Zhang et al., 2020). Furthermore, CAM6 misses the representation of several important mechanisms of secondary ice formation. Observed secondary ice formation processes include rime splintering, ice-ice collision fragmentation, droplet shattering during freezing, and fragmentation during sublimation of ice bridges (Field et al., 2017). Currently, only the rime splintering is considered in CAM6. Lastly, CAM6 with a horizontal resolution of approximately 100 km may not resolve the subgrid cloud processes and heterogeneous distributions of cloud hydrometeors (Tan et al., 2016; Zhang et al., 2019). These issues will be addressed in future studies.

删除了： other potential INP species, such as ash, biomass-burning particles, or other land-borne biological particles are not considered in the model currently.

5 Summary and Conclusions

This study introduces MOA into CAM6 as a new aerosol species and treats the chemistry, advection, and wet/dry deposition of MOA in the model. This paper also considers the MOA influences on droplet activation and ice nucleation, particularly focusing on quantifying the INP effect of MOA on cloud properties and radiation. Here we summarize our main findings:

(1) Three different emission schemes (B14, G11, and NULL) of MOA were implemented in the model and simulated MOA concentrations were evaluated with available observations. The global simulation indicates that high MOA burden centers are mostly co-located with regions of vigorous oceanic biological activities and high wind speeds such as in mid-latitude storm tracks, the equatorial upwelling, and coastal regions. The global MOA emission is 24.5 Tg yr^{-1} in B14, 27.1 Tg yr^{-1} in G11, and 4.6 Tg yr^{-1} in the NULL emission approach. On the global scale, the MOA mass emission is 0.67%, 0.74%, and 0.13% of the sea salt mass emission from B14, G11, and NULL, respectively. We show that observed seasonal cycles of marine organic matter at Mace Head and Amsterdam Island are reproduced when the MOA fraction of SSA is assumed to depend

on sea spray biology (B14, G11), but are not reproduced when this fraction is assumed to be constant (NULL). Our study does not support the constant organic mass fraction of SSA emissions (Quinn et al., 2014; Saliba et al., 2019; Bates et al., 2020).

(2) After introducing MOA in the model, annual mean CCN concentrations (at supersaturation of 0.1%) are increased by 15%–30% over the oceans ranging from 30°S to 70°S. Two different ice nucleation schemes of MOA (M18 and W15) are implemented and compared with available measurements. The INPs from MOA by the M18 parameterization show a reasonable agreement with observations at NH and SH high latitudes, while simulated total INPs, the sum of MOA INPs from M18 and dust INPs from D15, give a better agreement with observations. W15 for MOA alone overestimates the observed INP concentrations across all temperatures. At –25℃, MOA INP concentrations can be 1000 times higher than those of dust INPs over 40–60°S in the SH boundary layer while dust INP concentrations are higher above 400 hPa altitude over SH and NH.

(3) We notice a strong CCN effect of MOA over 40–60°S only in SH, while a strong INP effect of MOA is identified over 50–70° in both Hemispheres. For seasonal variations, CCN effect is stronger during the austral summer than winter, while INP effect is stronger in the austral winter than summer. The CCN effect of MOA on SWCF is strongest in the austral summer over SH with a value of –2.78 W m^{-2}, while the INP effect on LWCF is strongest in the austral winter over SH with a value of 0.35 W m^{-2}. The annual global mean CCN and INP effect of MOA on the net cloud forcing is –0.35 and 0.016 W m^{-2}, respectively. This work is a stepping stone towards better climate models because the important role of MOA in biogeochemistry, hydrological cycle, and climate change.

Competing interests: The authors declare that they have no conflict of interest.

Data availability: The model code is available at https://github.com/CESM-Development. The observed INP data is available at https://data.eol.ucar.edu/master_lists/generated/socrates/.

Author contributions: XZ and XL conceptualized the analysis and wrote the manuscript with input from the co-authors. XZ modified the code, carried out the simulations, and performed the analysis. SB provided scientific suggestions to the manuscript and provided the model code for the emission of marine organic aerosol. YS provided help in setting up the global climate model, designing the model runs, and created Figures. XL was involved with obtaining the project grant, supervised the study. All authors were involved in helpful discussions and contributed to the manuscript.

Acknowledgment: This research was supported by the DOE Atmospheric System Research (ASR) Program (grant DE-SC0020510). S. M. Burrows was also funded by the U.S. DOE Early Career Research Program. We thank Christina McCluskey for providing the INP data from the SOCRATES campaign.

References

Ault, A. P., Moffet, R. C., Baltrusaitis, J., Collins, D. B., Ruppel, M. J., Cuadra-Rodriguez, L. A., Zhao, D., Guasco, T. L., Ebben, C. J., Geiger, F. M., Bertram, T. H., Prather, K. A. and Grassian, V. H.: Size-dependent changes in sea spray aerosol composition and properties with different seawater conditions, Environmental Science and Technology, 47(11), 5603–5612, doi:10.1021/es400416g, 2013.

Abdul-Razzak, H., and Ghan, S. J.: A parameterization of aerosol activation 2. Multiple aerosol types, Journal of Geophysical Research Atmospheres, 105, 6837-6844, 10.1029/1999JD901161, 2000.

Alpert, P. A., Kilthau, W. P., Bothe, D. W., Radway, J. A. C., Aller, J. Y., and Knopf, D. A.: The influence of marine microbial activities on aerosol production: A laboratory mesocosm study, Journal of Geophysical Research, 120, 8841-8860, 10.1002/2015JD023469, 2015.

Ault, A. P., Moffet, R. C., Baltrusaitis, J., Collins, D. B., Ruppel, M. J., Cuadra-Rodriguez, L. A., Zhao, D., Guasco, T. L., Ebben, C. J., Geiger, F. M., Bertram, T. H., Prather, K. A., and Grassian, V. H.: Size-dependent changes in sea spray aerosol composition and properties with different seawater conditions, Environmental Science and Technology, 47, 5603-5612, 10.1021/es400416g, 2013.

Bates, T. S., Quinn, P. K., Coffman, D. J., Johnson, J. E., Upchurch, L., Saliba, G., Lewis, S., Graff, J., Russell, L. M., and Behrenfeld, M. J.: Variability in Marine Plankton Ecosystems Are Not Observed in Freshly Emitted Sea Spray Aerosol Over the North Atlantic Ocean, Geophys Res Lett, 47, 10.1029/2019GL085938, 2020.

Bigg, E. K.: The formation of atmospheric ice crystals by the freezing of droplets, Quarterly Journal of the Royal Meteorological Society, 79(342), 510–519, doi:10.1002/qj.49707934207, 1953.

Burrows, S. M., Easter, R., Liu, X., Ma, P. L., Wang, H., Elliott, S. M., Singh, B., Zhang, K., and Rasch, P. J.: OCEANFILMS sea-spray organic aerosol emissions – Part 1: implementation and impacts on clouds, Atmos. Chem. Phys. Discuss., 2018, 1-27, 10.5194/acp-2018-70, 2018.

Burrows, S. M., Ogunro, O., Frossard, A. A., Russell, L. M., Rasch, P. J., and Elliott, S. M.: A physically based framework for modeling the organic fractionation of sea spray aerosol from bubble film Langmuir equilibria, Atmos Chem Phys, 14, 13601-13629, 2014.

Ceburnis, D., O'Dowd, C. D., Jennings, G. S., Facchini, M. C., Emblico, L., Decesari, S., Fuzzi, S., and Sakalys, J.: Marine aerosol chemistry gradients: Elucidating primary and secondary processes and fluxes, Geophys Res Lett, 35, 2008.

Christiansen, S., Salter, M. E., Gorokhova, E., Nguyen, Q. T., and Bilde, M.: Sea Spray Aerosol Formation: Laboratory Results on the Role of Air Entrainment, Water Temperature, and Phytoplankton Biomass, Environmental Science and Technology, 10.1021/acs.est.9b04078, 2019.

Creamean, J. M., Kirpes, R. M., Pratt, K. A., Spada, N. J., Maahn, M., De Boer, G., Schnell, R. C., and China, S.: Marine and terrestrial influences on ice nucleating particles during continuous springtime measurements in an Arctic oilfield location, Atmos Chem Phys, 18, 18023-18042, 10.5194/acp-18-18023-2018, 2018.

Cullen, J. J.: The Deep Chlorophyll Maximum: Comparing Vertical Profiles of Chlorophyll a, Canadian Journal of Fisheries and Aquatic Sciences, 39, 791-803, 10.1139/f82-108, 1982.

D'Alessandro, J. J., Diao, M., Wu, C., Liu, X., Jensen, J. B., and Stephens, B. B.: Cloud phase and relative humidity distributions over the Southern Ocean in austral summer based on in situ observations and CAM5 simulations, Journal of Climate, 32, 2781-2805, 10.1175/JCLI-D-18-0232.1, 2019.

DeMott, P. J., Hill, T. C. J., McCluskey, C. S., Prather, K. A., Collins, D. B., Sullivan, R. C., Ruppel, M. J., Mason, R. H., Irish, V. E., Lee, T., Hwang, C. Y., Rhee, T. S., Snider, J. R., McMeeking, G. R., Dhaniyala, S., Lewis, E. R., Wentzell, J. J. B., Abbatt, J., Lee, C., Sultana, C. M., Ault, A. P., Axson, J. L., Martinez, M. D., Venero, I., Santos-Figueroa, G., Stokes, M. D., Deane, G. B., Mayol-Bracero, O.

L., Grassian, V. H., Bertram, T. H., Bertram, A. K., Moffett, B. F., and Franc, G. D.: Sea spray aerosol as a unique source of ice nucleating particles, P Natl Acad Sci USA, 113, 5797-5803, 2016.

DeMott, P. J., Prenni, A. J., McMeeking, G. R., Sullivan, R. C., Petters, M. D., Tobo, Y., Niemand, M., Mohler, O., Snider, J. R., Wang, Z., and Kreidenweis, S. M.: Integrating laboratory and field data to quantify the immersion freezing ice nucleation activity of mineral dust particles, Atmos Chem Phys, 15, 393-409, 2015.

Facchini, M. C., Rinaldi, M., Decesari, S., Carbone, C., Finessi, E., Mircea, M., Fuzzi, S., Ceburnis, D., Flanagan, R., Nilsson, E. D., de Leeuw, G., Martino, M., Woeltjen, J., and O'Dowd, C. D.: Primary submicron marine aerosol dominated by insoluble organic colloids and aggregates, Geophys Res Lett, 35, 10.1029/2008GL034210, 2008.

Field, P. R., Lawson, R. P., Brown, P. R. A., Lloyd, G., Westbrook, C., Moisseev, D., Miltenberger, A., Nenes, A., Blyth, A., Choularton, T., Connolly, P., Buehl, J., Crosier, J., Cui, Z., Dearden, C., DeMott, P., Flossmann, A., Heymsfield, A., Huang, Y., Kalesse, H., Kanji, Z. A., Korolev, A., Kirchgaessner, A., Lasher-Trapp, S., Leisner, T., McFarquhar, G., Phillips, V., Stith, J., and Sullivan, S.: Chapter 7. Secondary Ice Production - current state of the science and recommendations for the future, Meteorological Monographs, 58, 7.1-7.20, 10.1175/amsmonographs-d-16-0014.1, 2016.

Forestieri, S. D., Moore, K. A., Martinez Borrero, R., Wang, A., Stokes, M. D., and Cappa, C. D.: Temperature and Composition Dependence of Sea Spray Aerosol Production, Geophys Res Lett, 45, 7218-7225, 10.1029/2018GL078193, 2018.

Gantt, B., and Meskhidze, N.: The physical and chemical characteristics of marine primary organic aerosol: a review, Atmos Chem Phys, 13, 3979-3996, 2013.

Gantt, B., Meskhidze, N., Facchini, M. C., Rinaldi, M., Ceburnis, D., and O'Dowd, C. D.: Wind speed dependent size-resolved parameterization for the organic mass fraction of sea spray aerosol, Atmos Chem Phys, 11, 8777-8790, 2011.

Gantt, B., Xu, J., Meskhidze, N., Zhang, Y., Nenes, A., Ghan, S. J., Liu, X., Easter, R. and Zaveri, R.: Global distribution and climate forcing of marine organic aerosol – Part 2: Effects on cloud properties and radiative forcing, Atmospheric Chemistry and Physics, 12(14), 6555–6563, doi:10.5194/acp-12-6555-2012, 2012.

Gardner, W. D., Mishonov, A., and Richardson, M. J.: Global POC concentrations from in-situ and satellite data, Deep-Sea Res Pt Ii, 53, 718-740, 2006.

Gettelman, A., and Morrison, H.: Advanced Two-Moment Bulk Microphysics for Global Models. Part I: Off-Line Tests and Comparison with Other Schemes, Journal of Climate, 28, 1268-1287, 2015.

Golaz, J.-C., Larson, V. E., Cotton, W. R., Golaz, J.-C., Larson, V. E., and Cotton, W. R.: A PDF-Based Model for Boundary Layer Clouds. Part I: Method and Model Description, http://dx.doi.org/10.1175/1520-0469(2002)059<3540:APBMFB>2.0.CO;2, 10.1175/1520-0469(2002)059<3540:APBMFB>2.0.CO;2, 2002.

Golaz, J. C., Caldwell, P. M., Van Roekel, L. P., Petersen, M. R., Tang, Q., Wolfe, J. D., Abeshu, G., Anantharaj, V., Asay-Davis, X. S., Bader, D. C., Baldwin, S. A., Bisht, G., Bogenschutz, P. A., Branstetter, M., Brunke, M. A., Brus, S. R., Burrows, S. M., Cameron-Smith, P. J., Donahue, A. S., Deakin, M., Easter, R. C., Evans, K. J., Feng, Y., Flanner, M., Foucar, J. G., Fyke, J. G., Griffin, B. M., Hannay, C., Harrop, B. E., Hoffman, M. J., Hunke, E. C., Jacob, R. L., Jacobsen, D. W., Jeffery, N., Jones, P. W., Keen, N. D., Klein, S. A., Larson, V. E., Leung, L. R., Li, H. Y., Lin, W., Lipscomb, W. H., Ma, P. L., Mahajan, S., Maltrud, M. E., Mametjanov, A., McClean, J. L., McCoy, R. B., Neale, R. B., Price, S. F., Qian, Y., Rasch, P. J., Reeves Eyre, J. E. J., Riley, W. J., Ringler, T. D., Roberts, A. F., Roesler, E. L., Salinger, A. G., Shaheen, Z., Shi, X., Singh, B., Tang, J., Taylor, M. A., Thornton, P. E., Turner, A. K., Veneziani, M., Wan, H., Wang, H., Wang, S., Williams, D. N., Wolfram, P. J., Worley, P. H., Xie, S., Yang, Y., Yoon, J. H., Zelinka, M. D., Zender, C. S., Zeng, X., Zhang, C., Zhang, K., Zhang, Y., Zheng, X., Zhou, T., and Zhu, Q.: The DOE E3SM Coupled Model Version 1: Overview and Evaluation at Standard Resolution, Journal of Advances in Modeling Earth Systems, 11, 2089-2129, 10.1029/2018MS001603, 2019.

Hoose, C., Kristjánsson, J. E. and Burrows, S. M.: How important is biological ice nucleation in clouds on a global scale?, Environmental Research Letters, 5(2), 024009, doi:10.1088/1748-9326/5/2/024009, 2010.

Hoose, C., and Mohler, O.: Heterogeneous ice nucleation on atmospheric aerosols: a review of results from laboratory experiments, Atmos Chem Phys, 12, 9817-9854, 10.5194/acp-12-9817-2012, 2012.

Huang, W. T. K., Ickes, L., Tegen, I., Rinaldi, M., Ceburnis, D., and Lohmann, U.: Global relevance of marine organic aerosol as ice nucleating particles, Atmos Chem Phys, 18, 11423-11445, 2018.

Iacono, M. J., Delamere, J. S., Mlawer, E. J., Shephard, M. W., Clough, S. A., and Collins, W. D.: Radiative forcing by long-lived greenhouse gases: Calculations with the AER radiative transfer models, J Geophys Res-Atmos, 113, 2008.

Iacono, M. J., Delamere, J. S., Mlawer, E. J., Shephard, M. W., Clough, S. A., and Collins, W. D.: Radiative forcing by long-lived greenhouse gases: Calculations with the AER radiative transfer models, Journal of Geophysical Research Atmospheres, 113, 10.1029/2008JD009944, 2008.

Jahn, L. G., Polen, M. J., Jahl, L. G., Brubaker, T. A., Somers, J. and Sullivan, R. C.: Biomass combustion produces ice-active minerals in biomass-burning aerosol and bottom ash, Proceedings of the National Academy of Sciences of the United States of America, 117(36), 21928–21937, doi:10.1073/pnas.1922128117, 2020.

Kanji, Z. A., Ladino, L. A., Wex, H., Boose, Y., Burkert-Kohn, M., Cziczo, D. J., and Kramer, M.: Overview of Ice Nucleating Particles, Meteor Mon, 58, 10.1175/Amsmonographs-D-16-0006.1, 2017.

Langmann, B., Scannell, C., and O'Dowd, C.: New Directions: Organic matter contribution to marine aerosols and cloud condensation nuclei, Atmos Environ, 42, 7821-7822, 2008.

Larson, V. E., Golaz, J.-C., and Cotton, W. R.: Small-Scale and Mesoscale Variability in Cloudy Boundary Layers: Joint Probability Density Functions, Journal of the Atmospheric Sciences, 59, 3519-3539, 10.1175/1520-0469(2002)059<3519:SSAMVI>2.0.CO;2, 2002.

Lin, S. J., and Rood, R. B.: An explicit flux-form semi-Lagrangian shallow-water model on the sphere, Q J Roy Meteor Soc, 123, 2477-2498, 1997.

Liu, X., Easter, R. C., Ghan, S. J., Zaveri, R., Rasch, P., Shi, X., Lamarque, J. F., Gettelman, A., Morrison, H., Vitt, F., Conley, A., Park, S., Neale, R., Hannay, C., Ekman, A. M. L., Hess, P., Mahowald, N., Collins, W., Iacono, M. J., Bretherton, C. S., Flanner, M. G., and Mitchell, D.: Toward a minimal representation of aerosols in climate models: description and evaluation in the Community Atmosphere Model CAM5, Geosci Model Dev, 5, 709-739, 2012.

Liu, X., Ma, P. L., Wang, H., Tilmes, S., Singh, B., Easter, R. C., Ghan, S. J., and Rasch, P. J.: Description and evaluation of a new four-mode version of the Modal Aerosol Module (MAM4) within version 5.3 of the Community Atmosphere Model, Geosci Model Dev, 9, 505-522, 2016.

Martensson, E. M., Nilsson, E. D., de Leeuw, G., Cohen, L. H., and Hansson, H. C.: Laboratory simulations and parameterization of the primary marine aerosol production, J Geophys Res-Atmos, 108, 2003.

McCluskey, C. S., DeMott, P. J., Ma, P. L., and Burrows, S. M.: Numerical Representations of Marine Ice-Nucleating Particles in Remote Marine Environments Evaluated Against Observations, Geophys Res Lett, 46, 7838-7847, 10.1029/2018gl081861, 2019.

McCluskey, C. S., Hill, T. C. J., Humphries, R. S., Rauker, A. M., Moreau, S., Strutton, P. G., Chambers, S. D., Williams, A. G., McRobert, I., Ward, J., Keywood, M. D., Harnwell, J., Ponsonby, W., Loh, Z. M., Krummel, P. B., Protat, A., Kreidenweis, S. M., and DeMott, P. J.: Observations of Ice Nucleating Particles Over Southern Ocean Waters, Geophys Res Lett, 45, 11,989-911,997, 10.1029/2018GL079981, 2018a.

McCluskey, C. S., Ovadnevaite, J., Rinaldi, M., Atkinson, J., Belosi, F., Ceburnis, D., Marullo, S., Hill, T. C. J., Lohmann, U., Kanji, Z. A., O'Dowd, C., Kreidenweis, S. M., and DeMott, P. J.: Marine and

Terrestrial Organic Ice-Nucleating Particles in Pristine Marine to Continentally Influenced Northeast Atlantic Air Masses, J Geophys Res-Atmos, 123, 6196-6212, 2018b.

Meskhidze, N., Xu, J., Gantt, B., Zhang, Y., Nenes, A., Ghan, S. J., Liu, X., Easter, R., and Zaveri, R.: Global distribution and climate forcing of marine organic aerosol: 1. Model improvements and evaluation, Atmos Chem Phys, 11, 11689-11705, 2011.

Meyers, M. P., Demott, P. J. and Cotton, W. R.: New primary ice-nucleation parameterizations in an explicit cloud model, Journal of Applied Meteorology, 31(7), 708–721, doi:10.1175/1520-0450(1992)031<0708:NPINPI>2.0.CO;2, 1992.

Mlawer, E. J., Taubman, S. J., Brown, P. D., Iacono, M. J., and Clough, S. A.: Radiative transfer for inhomogeneous atmospheres: RRTM, a validated correlated-k model for the longwave, J Geophys Res-Atmos, 102, 16663-16682, 1997.

Murray, B. J., O'Sullivan, D., Atkinson, J. D., and Webb, M. E.: Ice nucleation by particles immersed in supercooled cloud droplets, Chem Soc Rev, 41, 6519-6554, 10.1039/c2cs35200a, 2012.

Niemand, M., Möhler, O., Vogel, B., Vogel, H., Hoose, C., Connolly, P., Klein, H., Bingemer, H., DeMott, P., Skrotzki, J., and Leisner, T.: A Particle-Surface-Area-Based Parameterization of Immersion Freezing on Desert Dust Particles, Journal of the Atmospheric Sciences, 69, 3077-3092, 10.1175/JAS-D-11-0249.1, 2012.

O'Dowd, C. D., Facchini, M. C., Cavalli, F., Ceburnis, D., Mircea, M., Decesari, S., Fuzzi, S., Yoon, Y. J., and Putaud, J. P.: Biogenically driven organic contribution to marine aerosol, Nature, 431, 676-680, 2004.

O'Dowd, C. D., Langmann, B., Varghese, S., Scannell, C., Ceburnis, D., and Facchini, M. C.: A combined organic-inorganic sea-spray source function, Geophys Res Lett, 35, 2008.

Prather, K. A., Bertram, T. H., Grassian, V. H., Deane, G. B., Stokes, M. D., DeMott, P. J., Aluwihare, L. I., Palenik, B. P., Azam, F., Seinfeld, J. H., Moffet, R. C., Molina, M. J., Cappa, C. D., Geiger, F. M., Roberts, G. C., Russell, L. M., Ault, A. P., Baltrusaitis, J., Collins, D. B., Corrigan, C. E., Cuadra-Rodriguez, L. A., Ebben, C. J., Forestieri, S. D., Guasco, T. L., Hersey, S. P., Kim, M. J., Lambert, W. F., Modini, R. L., Mui, W., Pedler, B. E., Ruppel, M. J., Ryder, O. S., Schoepp, N. G., Sullivan, R. C., and Zhao, D.: Bringing the ocean into the laboratory to probe the chemical complexity of sea spray aerosol, P Natl Acad Sci USA, 110, 7550-7555, 10.1073/pnas.1300262110, 2013.

Quinn, P. K., Bates, T. S., Schulz, K. S., Coffman, D. J., Frossard, A. A., Russell, L. M., Keene, W. C., and Kieber, D. J.: Contribution of sea surface carbon pool to organic matter enrichment in sea spray aerosol, Nat Geosci, 7, 228-232, 10.1038/ngeo2092, 2014.

Rasch, P. J., Xie, S., Ma, P. L., Lin, W., Wang, H., Tang, Q., Burrows, S. M., Caldwell, P., Zhang, K., Easter, R. C., Cameron-Smith, P., Singh, B., Wan, H., Golaz, J. C., Harrop, B. E., Roesler, E., Bacmeister, J., Larson, V. E., Evans, K. J., Qian, Y., Taylor, M., Leung, L. R., Zhang, Y., Brent, L., Branstetter, M., Hannay, C., Mahajan, S., Mametjanov, A., Neale, R., Richter, J. H., Yoon, J. H., Zender, C. S., Bader, D., Flanner, M., Foucar, J. G., Jacob, R., Keen, N., Klein, S. A., Liu, X., Salinger, A. G., Shrivastava, M., and Yang, Y.: An Overview of the Atmospheric Component of the Energy Exascale Earth System Model, Journal of Advances in Modeling Earth Systems, 11, 2377-2411, 10.1029/2019MS001629, 2019.

Rastelli, E., Corinaldesi, C., Dell'anno, A., Lo Martire, M., Greco, S., Cristina Facchini, M., Rinaldi, M., O'Dowd, C., Ceburnis, D., and Danovaro, R.: Transfer of labile organic matter and microbes from the ocean surface to the marine aerosol: An experimental approach, Sci Rep-Uk, 7, 1-10, 10.1038/s41598-017-10563-z, 2017.

Rinaldi, M., Fuzzi, S., Decesari, S., Marullo, S., Santoleri, R., Provenzale, A., von Hardenberg, J., Ceburnis, D., Vaishya, A., O'Dowd, C. D., and Facchini, M. C.: Is chlorophyll-a the best surrogate for organic matter enrichment in submicron primary marine aerosol?, J Geophys Res-Atmos, 118, 4964-4973, 2013.

Saliba, G., Chen, C. L., Lewis, S., Russell, L. M., Rivellini, L. H., Lee, A. K. Y., Quinn, P. K., Bates, T. S., Haëntjens, N., Boss, E. S., Karp-Boss, L., Baetge, N., Carlson, C. A., and Behrenfeld, M. J.: Factors driving the seasonal and hourly variability of sea-spray aerosol number in the North Atlantic, P Natl Acad Sci USA, 116, 20309-20314, 10.1073/pnas.1907574116, 2019.

Schnell, R. C., and Vali, G.: Freezing nuclei in marine waters, Tellus, 27, 321-323, 10.3402/tellusa.v27i3.9911, 1975.

Schill, G. P., DeMott, P. J., Emerson, E. W., Rauker, A. M. C., Kodros, J. K., Suski, K. J., Hill, T. C. J., Levin, E. J. T., Pierce, J. R., Farmer, D. K. and Kreidenweis, S. M.: The contribution of black carbon to global ice nucleating particle concentrations relevant to mixed-phase clouds, Proceedings of the National Academy of Sciences of the United States of America, 117(37), 22705–22711, doi:10.1073/pnas.2001674117, 2020.

Sciare, J., Favez, O., Sarda-Esteve, R., Oikonomou, K., Cachier, H., and Kazan, V.: Long-term observations of carbonaceous aerosols in the Austral Ocean atmosphere: Evidence of a biogenic marine organic source, J Geophys Res-Atmos, 114, 2009.

Shi, Y., and Liu, X.: Dust Radiative Effects on Climate by Glaciating Mixed-Phase Clouds, Geophys Res Lett, 46, 6128-6137, 10.1029/2019GL082504, 2019.

Steele, J. H.: ENVIRONMENTAL CONTROL OF PHOTOSYNTHESIS IN THE SEA, Limnology and Oceanography, 7, 137-150, 10.4319/lo.1962.7.2.0137, 1962.

Tobo, Y., Adachi, K., DeMott, P. J., Hill, T. C. J., Hamilton, D. S., Mahowald, N. M., Nagatsuka, N., Ohata, S., Uetake, J., Kondo, Y., and Koike, M.: Glacially sourced dust as a potentially significant source of ice nucleating particles, Nat Geosci, 12, 253-+, 10.1038/s41561-019-0314-x, 2019.

Vali, G., DeMott, P. J., Möhler, O. and Whale, T. F.: Technical Note: A proposal for ice nucleation terminology, Atmospheric Chemistry and Physics, 15(18), 10263–10270, doi:10.5194/acp-15-10263-2015, 2015.

Vergara-Temprado, J., Murray, B. J., Wilson, T. W., O'Sullivan, D., Browse, J., Pringle, K. J., Ardon-Dryer, K., Bertram, A. K., Burrows, S. M., Ceburnis, D., DeMott, P. J., Mason, R. H., O'Dowd, C. D., Rinaldi, M., and Carslaw, K. S.: Contribution of feldspar and marine organic aerosols to global ice nucleating particle concentrations, Atmos Chem Phys, 17, 3637-3658, 2017.

Vergara-Temprado, J., Holden, M. A., Orton, T. R., O'Sullivan, D., Umo, N. S., Browse, J., Reddington, C., Baeza-Romero, M. T., Jones, J. M., Lea-Langton, A., Williams, A., Carslaw, K. S. and Murray, B. J.: Is Black Carbon an Unimportant Ice-Nucleating Particle in Mixed-Phase Clouds?, Journal of Geophysical Research: Atmospheres, 123(8), 4273–4283, doi:10.1002/2017JD027831, 2018.

Vignati, E., Facchini, M. C., Rinaldi, M., Scannell, C., Ceburnis, D., Sciare, J., Kanakidou, M., Myriokefalitakis, S., Dentener, F., and O'Dowd, C. D.: Global scale emission and distribution of sea-spray aerosol: Sea-salt and organic enrichment, Atmos Environ, 44, 670-677, 2010.

Wang, X., Deane, G. B., Moore, K. A., Ryder, O. S., Stokes, M. D., Beall, C. M., Collins, D. B., Santander, M. V., Burrows, S. M., Sultana, C. M., and Prather, K. A.: The role of jet and film drops in controlling the mixing state of submicron sea spray aerosol particles, P Natl Acad Sci USA, 114, 6978-6983, 10.1073/pnas.1702420114, 2017.

Wang, Y., Liu, X., Hoose, C., and Wang, B.: Different contact angle distributions for heterogeneous ice nucleation in the Community Atmospheric Model version 5, Atmos Chem Phys, 14, 10411-10430, 2014.

Wilson, T. W., Ladino, L. A., Alpert, P. A., Breckels, M. N., Brooks, I. M., Browse, J., Burrows, S. M., Carslaw, K. S., Huffman, J. A., Judd, C., Kilthau, W. P., Mason, R. H., McFiggans, G., Miller, L. A., Najera, J. J., Polishchuk, E., Rae, S., Schiller, C. L., Si, M., Temprado, J. V., Whale, T. F., Wong, J. P. S., Wurl, O., Yakobi-Hancock, J. D., Abbatt, J. P. D., Aller, J. Y., Bertram, A. K., Knopf, D. A., and Murray, B. J.: A marine biogenic source of atmospheric ice-nucleating particles, Nature, 525, 234-+, 2015.

Wolf, M. J., Coe, A., Dove, L. A., Zawadowicz, M. A., Dooley, K., Biller, S. J., Zhang, Y., Chisholm, S. W., and Cziczo, D. J.: Investigating the Heterogeneous Ice Nucleation of Sea Spray Aerosols Using Prochlorococcus as a Model Source of Marine Organic Matter, Environmental Science and Technology, 53, 1139-1149, 10.1021/acs.est.8b05150, 2019.

Yoon, Y. J., Ceburnis, D., Cavalli, F., Jourdan, O., Putaud, J. P., Facchini, M. C., Decesari, S., Fuzzi, S., Sellegri, K., Jennings, S. G., and O'Dowd, C. D.: Seasonal characteristics of the physicochemical properties of North Atlantic marine atmospheric aerosols, Journal of Geophysical Research Atmospheres, 112, 10.1029/2005JD007044, 2007.

Yun, Y. X., and Penner, J. E.: An evaluation of the potential radiative forcing and climatic impact of marine organic aerosols as heterogeneous ice nuclei, Geophys Res Lett, 40, 4121-4126, 2013.

Zhang, G. J., and Mcfarlane, N. A.: Sensitivity of Climate Simulations to the Parameterization of Cumulus Convection in the Canadian Climate Center General-Circulation Model, Atmos Ocean, 33, 407-446, 1995.

Zhang, M., Liu, X., Diao, M., D'Alessandro, J. J., Wang, Y., Wu, C., Zhang, D., Wang, Z., and Xie, S.: Impacts of Representing Heterogeneous Distribution of Cloud Liquid and Ice on Phase Partitioning of Arctic Mixed-Phase Clouds with NCAR CAM5, Journal of Geophysical Research: Atmospheres, 124, 13071-13090, 10.1029/2019JD030502, 2019.

Zhang, M., Xie, S., Liu, X., Lin, W., Zhang, K., Ma, H. Y., Zheng, X., and Zhang, Y.: Toward Understanding the Simulated Phase Partitioning of Arctic Single-Layer Mixed-Phase Clouds in E3SM, Earth and Space Science, 10.1029/2020ea001125, 2020.

Table 1. Aerosol species in MAM4 modes

	Accumulation	**Aitken**	**Coarse**	**Primary Carbon**
Species[1]	num_a1, so4_a1, pom_a1, soa_a1, bc_a1, dst_a1, ncl_a1, moa_a1	num_a2, so4_a2, soa_a2, ncl_a2, dst_a2, moa_a2	num_a3, dst_a3, ncl_a3, so4_a3	num_a4, pom_a4, bc_a4, (moa_a4 if externally added)
Size range	0.08 – 1 μm	0.02 – 0.08 μm	1–10 μm	0.08 - 1 μm
Standard Deviation σg	1.6	1.6	1.2	1.6
Number-median diameter *Dgn*	1.1×10^{-7}	2.6×10^{-8}	2.0×10^{-6}	5.0×10^{-8}
Low bound *Dgn*	5.35×10^{-8}	8.7×10^{-9}	4.0×10^{-7}	1.0×10^{-8}
High bound *Dgn*	4.8×10^{-7}	5.2×10^{-8}	4.0×10^{-5}	1.0×10^{-7}

[1]so4_aX: sulfate mass mixing ratio in mode X; pom_aX: particulate organic matter (POM) mass mixing ratio in mode X; soa_aX: secondary organic aerosol (SOA) mass mixing ratio in mode X; bc_aX: black carbon (BC) mass mixing ratio in mode X; dst_aX: dust mass mixing ratio in mode X; ncl_aX: sea salt mass mixing ratio in mode X; moa_aX: marine organic aerosol (MOA) mass mixing ratio in mode X; and num_aX: number mixing ratio of mode X. *_a1: accumulation mode; *_a2: Aitken mode; *_a3: coarse mode; and *_a4: coarse mode.

删除了：**p**

删除了：num_a3, dst_a3, ncl_a3, so4_a3SOA, DST, NCL

设置了格式：字体颜色：文字 1，上标

删除了：num_a2, so4_a2, soa_a2, ncl_a2, dst_a2, mom_a2SO4, SOA, DST, NCL, MOA

删除了：POA, BCnum_a4, pom_a4, bc_a4, (mom_a4MOA if internal added)

删除了：num_a1, so4_a1, pom_a1, soa_a1, bc_a1, dst_a1, ncl_a1, mom_a1 SO4, POA, SOA, BC, DST, NCL, MOA

带格式的：居中

删除了：* → SO4 represents sulfate; POA represents primary organic; SOA represents secondary organic; BC is black carbon; DST is dust; NCl represents sea salt; MOA represents marine organic aerosol. ↵

带格式的：左

Table 2. Aerosol species and physical properties

Species	Name	Density (kg m^{-3})	Hygroscopicity
BC	Black carbon	1700	1.0×10^{-10}
SO4	Sulfate	1770	0.507
SOA	Secondary organic	1000	0.14
POA	Primary organic	1000	1.0×10^{-10}
DST	Dust	2600	0.068
NCL	Sea salt	1900	1.16
MOA	Marine organic aerosol	1601	0.1

Table 3. Molecular weights, mass at saturation, Langmuir parameters of the three ocean macromolecules

Species	**polysaccharides**	**proteins**	**Lipids**
Molecular weight [g mol^{-1}]	250000	66463	284
mass per area at saturation [g m^{-2}]	0.1376	0.00219	0.002593
Langmuir parameter [m^3 mol^{-1}]	90.58	25175	18205

Table 4. List of experiments to test model sensitivity to different emission and ice nucleation schemes

Name	Emission of MOA	DUST ice nucleation	MOA ice nucleation	Notes
BASE	—	CNT	—	Base line simulation
B14	Burrows et al. [2014]	CNT	—	Sensitivity test of emission scheme
G11	Gantt et al. [2011]	CNT	—	Sensitivity test of emission scheme
NULL	NULL	CNT	—	Sensitivity test of emission scheme
CTL		DeMott et al. [2015]		Control simulation
B14_D15	Burrows et al. [2014]	DeMott et al. [2015]		CCN effect
B14_D15_M18	Burrows et al. [2014]	DeMott et al. [2015]	McCluskey et al. [2018]	INP effect
B14_D15_W15	Burrows et al. [2014]	DeMott et al. [2015]	Wilson et al. [2015]	Sensitivity test of MOA INP parameterization
B14_N12_M18	Burrows et al. [2014]	Niemand et al. [2012]	McCluskey et al. [2018]	Sensitivity test of dust INP parameterization
B14_CNT_M18	Burrows et al. [2014]	CNT	McCluskey et al. [2018]	Sensitivity test of dust INP parameterization

Table 5. Annual global mean emissions and burdens of MOA and sea salt

Name	Sea salt emission ($Tg\ yr^{-1}$)	MOA emission ($Tg\ yr^{-1}$)	Sea salt burden (Tg)	MOA burden (Tg)	MOA/Sea salt emission (%)
BASE	3651	—	8.83	—	—
B14	3656	24.5	8.88	0.097	0.67
G11	3666	27.1	8.86	0.120	0.74
NULL	3648	4.6	8.85	0.018	0.13

Table 6. Mean changes and relative changes (%) between CTL and B14_D15_M18 experiments. Included in the table are surface CCN concentrations at 0.1% (CCN), ice particle number concentration at –15ºC thermal level (Ni_15), vertically-integrated cloud droplet number concentration (CDNUMC), total grid-box cloud liquid water path (LWP), total grid-box cloud ice water path (IWP), shortwave and longwave cloud forcings (SWCF, LWCF), total cloud fraction (CLDTOT), high/mid-level/low-level clouds (CLDHGH, CLDMED, CLDLOW), and total surface precipitation rate (PRECT), with bold fond indicating relative changes larger than 3%.

	Global ANN	20S–90S ANN	20S–90S JJA	20S–90S DJF
CCN (cm^{-3})	**3.28 (3.17)**	**4.85 (8.45)**	1.37 (2.84)	**9.26 (13.47)**
Ni_15 (m^{-3})	39.39 (2.25)	**102.0 (5.21)**	**275.93 (9.34)**	–3.05 (–0.510)
CDNUMC (cm^{-2})	$\mathbf{7.53 \times 10^4}$ **(5.25)**	$\mathbf{1.27 \times 10^5}$ **(8.65)**	1.10×10^4 (0.94)	$\mathbf{3.22 \times 10^5}$ **(16.89)**
LWP ($g\ m^{-2}$)	0.69 (1.02)	0.66 (0.77)	–1.86 (–2.32)	**4.57 (5.10)**
IWP ($g\ m^{-2}$)	0.05 (0.37)	0.10 (0.99)	0.42 (3.69)	0.13 (1.48)
SWCF ($W\ m^{-2}$)	–0.41 (0.86)	–0.63 (1.17)	0.400 (–1.48)	**–2.87 (3.47)**
LWCF ($W\ m^{-2}$)	0.08 (0.35)	0.031 (0.15)	0.13 (0.57)	0.11 (0.52)
CLDTOT (%)	0.12 (0.17)	0.17 (0.22)	0.011 (0.014)	1.05 (1.45)
CLDHGH (%)	0.016 (0.039)	–0.0082 (–0.021)	–0.027 (–0.071)	–0.18 (–0.47)
CLDMED (%)	0.078 (0.26)	0.19 (0.55)	0.20 (0.54)	0.017 (0.054)
CLDLOW (%)	0.13 (0.33)	0.14 (0.24)	–0.43 (–0.69)	1.35 (2.52)
PRECT ($mm\ day^{-1}$)	–0.0011 (–0.038)	0.0042 (0.17)	0.019 (0.71)	0.040 (1.66)

Table 7. CCN and INP effects of MOA on SWCF, and the values in the table are the mean change and relative change (%). The CCN effect is calculated between CTL and B14_D15 experiments, and the INP effect is calculated between B14_D15 and B14D15_M18 experiments, with the bold font indicated the maximum change.

		ANN	MAM	JJA	SON	DJF
20–90S	CCN	–0.84 (1.58)	–0.47 (1.16)	0.48 (–1.78)	–0.59 (0.95)	**–2.78 (3.36)**
	INP	0.22 (–0.50)	0.084 (–0.20)	–0.080 (0.30)	0.94 (–1.51)	–0.088 (0.10)
global	CCN	–0.41 (0.85)	–0.21 (0.48)	–0.43 (0.89)	0.027 (–0.056)	–1.01 (1.96)
	INP	–0.0037 (0.0077)	0.047 (–0.11)	0.27 (–0.54)	–0.16 (0.33)	–0.17 (0.33)

Table 8. CCN and INP effect of MOA on LWCF, and the values in the table are the mean change and relative change (%). The CCN effect is calculated between CTL and B14_D15 experiments, and the INP effect is calculated between B14_D15 and B14D15_M18 experiments, with the bold fond indicated the maximum change.

		ANN	MAM	JJA	SON	DJF
20–90S	CCN	0.064 (0.30)	0.033 (0.15)	–0.21 (–0.93)	0.29 (1.39)	0.15 (0.73)
	INP	–0.033 (–0.15)	–0.15 (–0.68)	**0.35 (1.5)**	–0.29 (–1.35)	–0.042 (–0.20)
global	CCN	0.064 (0.27)	–0.0097 (–0.040)	–0.032 (–0.13)	0.0890 (0.38)	0.21 (0.91)
	INP	0.020 (0.085)	–0.12 (–0.50)	0.21 (0.85)	0.035 (0.15)	–0.039 (–0.17)

Figures

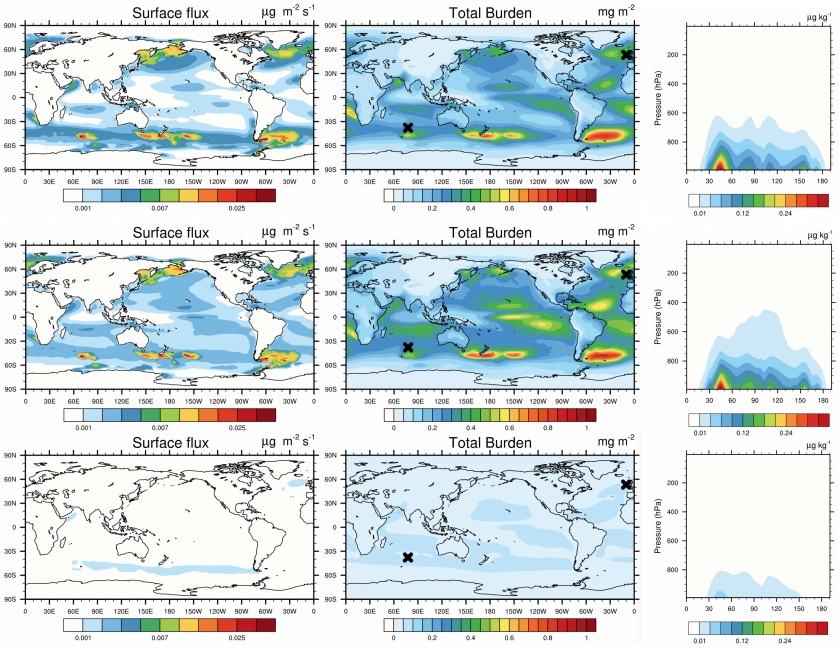

Figure 1. Spatial distributions of annual mean surface flux (first column, in unit of μg m^{-2} s^{-1}) and vertically-integrated (column) burden of MOA (second column, in unit of mg m^{-2}), and latitude-pressure cross-sections of annual mean MOA mixing ratio (third column, in unit of μg kg^{-1}) from the B14 (first row), G11 (second row), and NULL (third row) experiments. The right black cross in the second row indicates the position of Mace Head, and the left black cross indicates the position of Amsterdam Island.

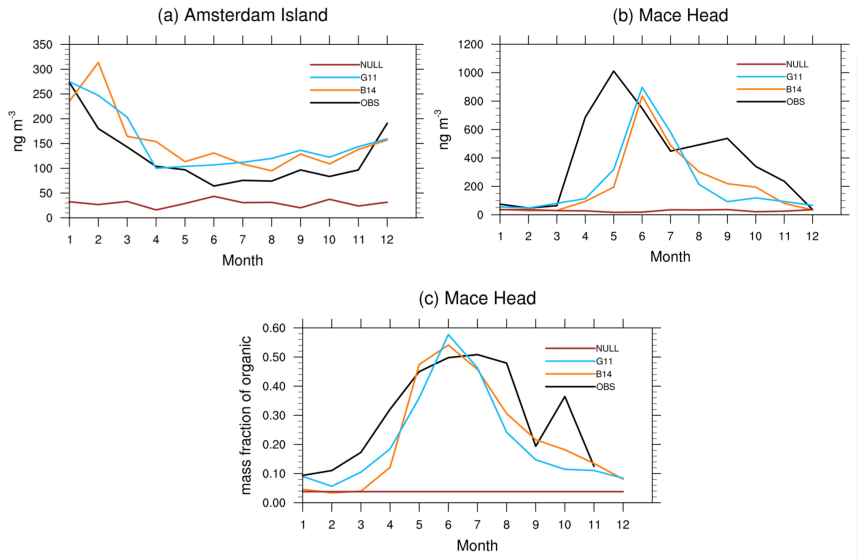

Figure 2. Monthly averaged concentrations of MOA at (a) Amsterdam Island and (b) Mace Head Ireland; and (c) monthly averaged mass fraction of MOA in SSA at Mace Head Ireland. The locations of Amsterdam Island and Mace Head Ireland are shown in Figure 1.

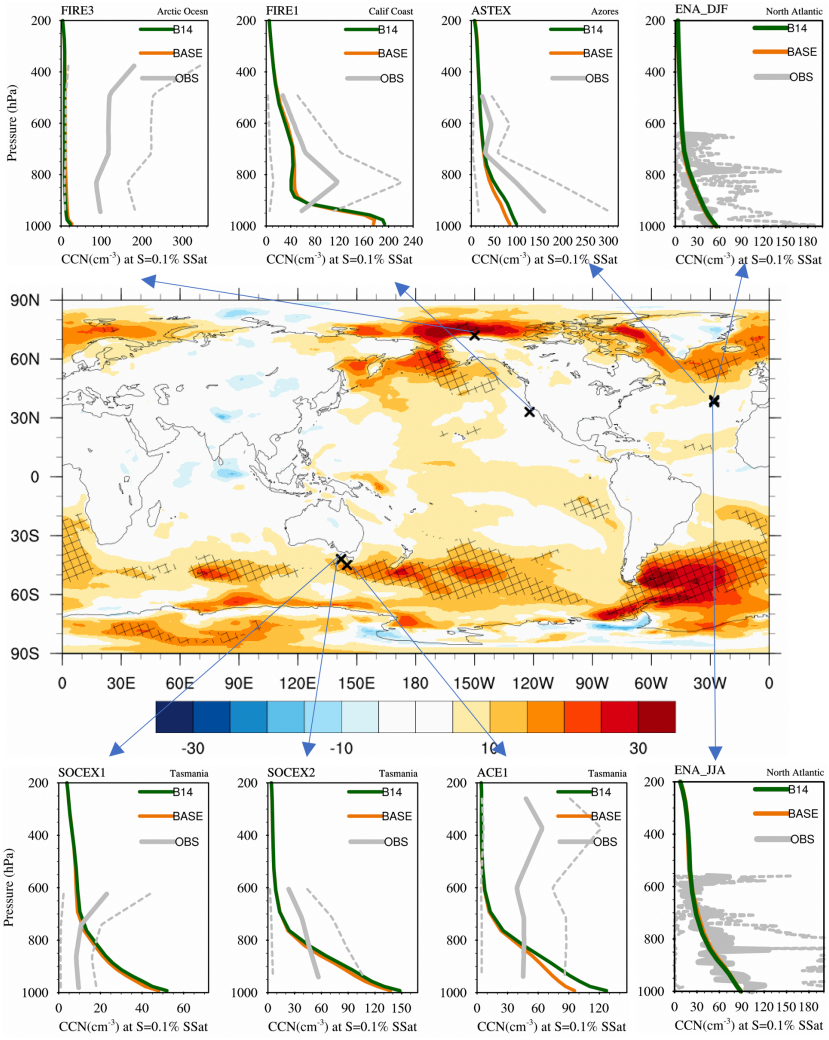

Figure 3. Spatial distribution of annual mean percentage changes of surface CCN concentrations at 0.1% supersaturation due to MOA (by comparing B14_D15 and BASE), and vertical distribution of CCN concentrations at 0.1% supersaturation from eight measurements (solid gray lines), BASE (solid orange line) and B14_D15 (solid green line). Dashed lines outline a range of 10th and 90th percentiles for measurements in different field campaigns: FIRE1 (the First International Satellite Cloud Climatology Project Reginal Experiment) locates at 33° N and 238° E in California coast, the data is collected during June to July, 1987; the FIRE3 locates at 72° N and 210° E in Arctic Ocean, the data is collected during May, 1998; the ASTEX (Atlantic Stratocumulus Transition Experiment) locates at 38° N and 332° E in Azores, the data is collected during June, 1992; the SOCEX1 (Southern Ocean Cloud Experiment) is located as –42 ° S and 142° E in Tasmania, the data is collected during July 1993; the data of SOCEX2 is collected during

删除了： Figure 3. Spatial distribution of annual mean percentage changes of surface CCN concentrations at 0.1% supersaturation due to MOA, and vertical distribution of CCN concentrations at 0.1% supersaturation from eight measurements (solid gray lines), BASE (solid orange line) and B14_D15 (solid green line). Dashed lines outline a range

删除了： W

删除了： W

删除了： W

January to February 1995; the ACE1 (Aerosol Characterization Experiment) locates at –45 ° S , 145° E in Tasmania, the data is collected during November to December, 1995; and the ENA_JJA(Eastern North Atlantic) locates at 39° N and 332° E in Eastern North Atlantic, the data is collected during June to August, while ENA_DJF is collected during December, January, and February, 2006 to 2020.

删除了：W

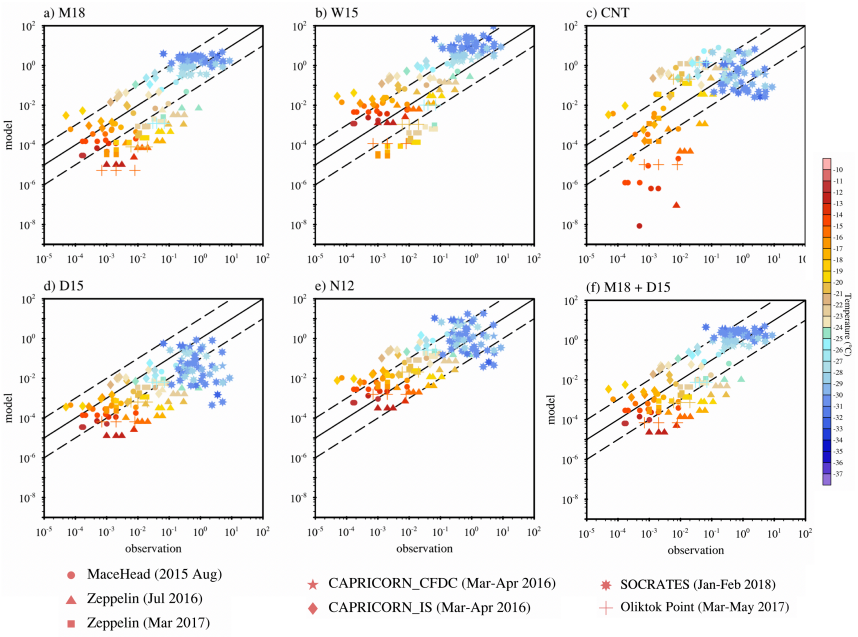

Figure 4. Comparison of simulated vs. observed INP number concentrations for different simulations: (a) MOA INPs from M18 [McCluskey et al., 2018], (b) MOA INPs from W15 [Wilson et al., 2015], (c) dust INPs from CNT [Wang et al., 2014], (d) dust INPs from D15 [DeMott et al., 2015], (e) dust INPs from N12 [Niemand et al., 2012], and (f) sum of dust and MOA INPs from D15 and M18. Simulated INPs data are sampled at the same pressures, longitudes and latitudes as the field measurements. Dashed lines outline a factor of 10 about the 1:1 line (solid) in all the panels. Color bar shows the observed temperature in °C, while different markers represent different field campaigns. Zeppelin site locates at 78.9081° N, 11.8814° E, 475 m above mean sea level in NyÅlesund, Svalbard, the INP data is collected during July 2016 and March 2017 [Tobo et al., 2019]; Oliktok Point site locates at 70.50° N 149.89°W, the INP data is collected during March-May 2017 [Creamean et al., 2018)]; CAPRICORN (Clouds, Aerosols, Precipitation, Radiation, and Atmospheric Composition over the Southern Ocean) INP data is collected on ships during 13 March to 15 April in 2016 over the Southern Ocean [McCluskey, Hill, Humphries, et al., 2018a]; Mace Head site locates at 53.32°N, 9.90°W, the INP data is collected during August 2015 [McCluskey, Ovadnevaite, Rinaldi, et al., 2018b]; SOCRATES (Southern Ocean Clouds, Radiation, Aerosol Transport Experimental Study) INP data is collected on flights during January-February 2018 over the Southern Ocean by Paul DeMott (https://data.eol.ucar.edu/master_lists/generated/socrates/).

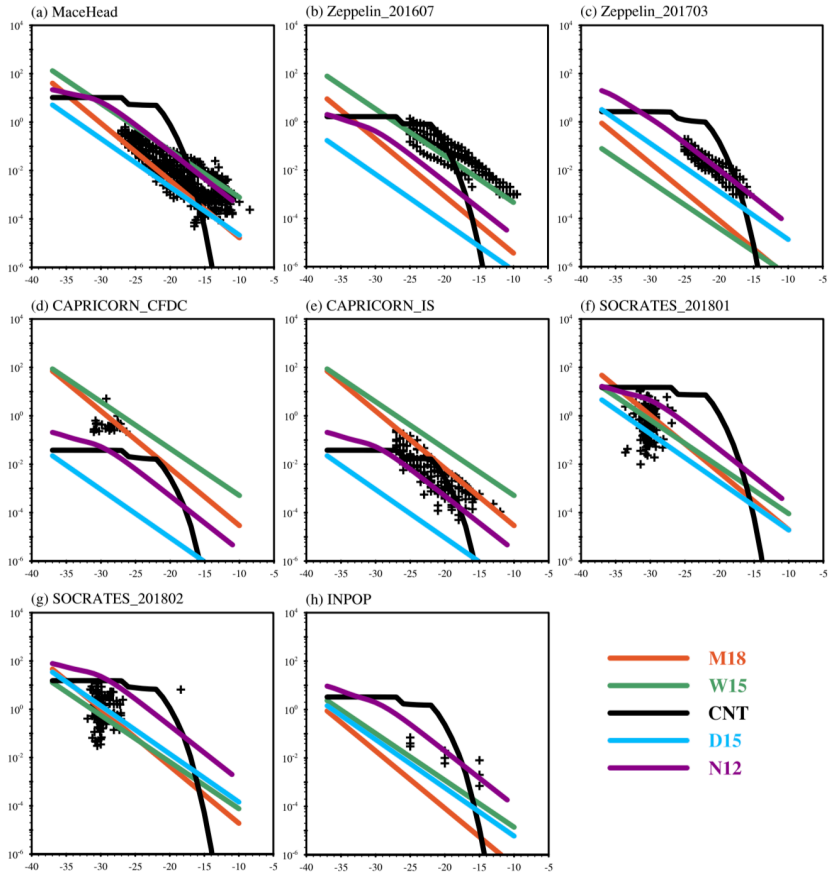

Figure 5. Modeled and observed INP concentrations as a function of temperature. The black crosses indicate INP measurements, and lines show model results from different parameterizations (Table 4). Simulated INPs data are sampled at the same pressures, longitudes and latitudes as the field measurements.

删除了： Model grid points are selected at the same pressure levels and longitudes and latitudes as field measurements.

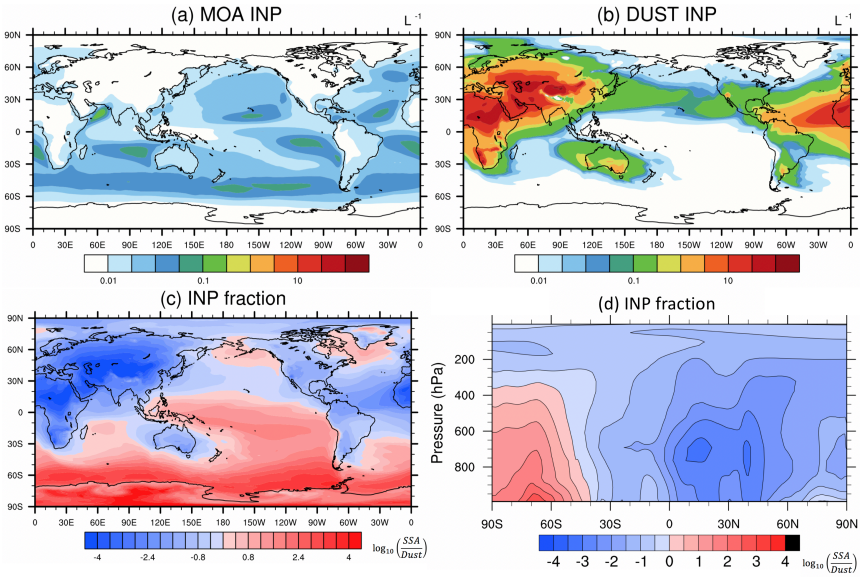

Figure 6. Spatial distribution of annual mean concentrations of (a) MOA INPs, (b) dust INPs, and (c) ratio of MOA INP concentration to dust INP concentration at 950 hPa, and (d) vertical cross sections of ratio of MOA INP concentration to dust INP concentration. INP concentrations are diagnosed at temperature of –25℃.

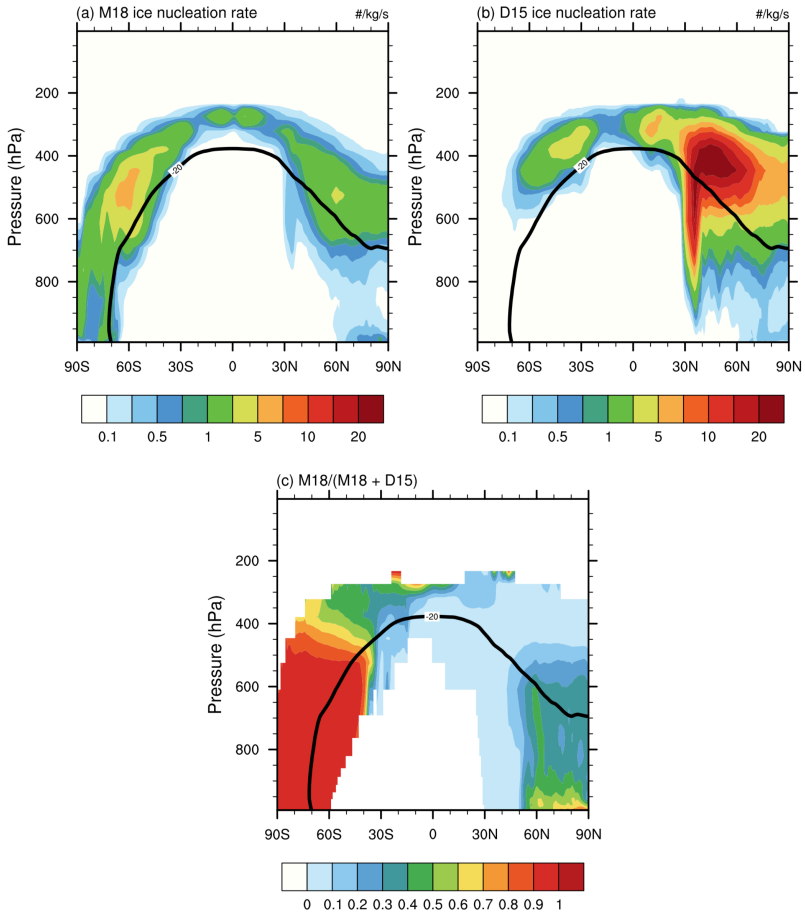

Figure 7. Annual zonal mean pressure-latitude cross sections of ice nucleation rates from (a) MOA, (b) dust, and (c) MOA fraction of total ice production rate.

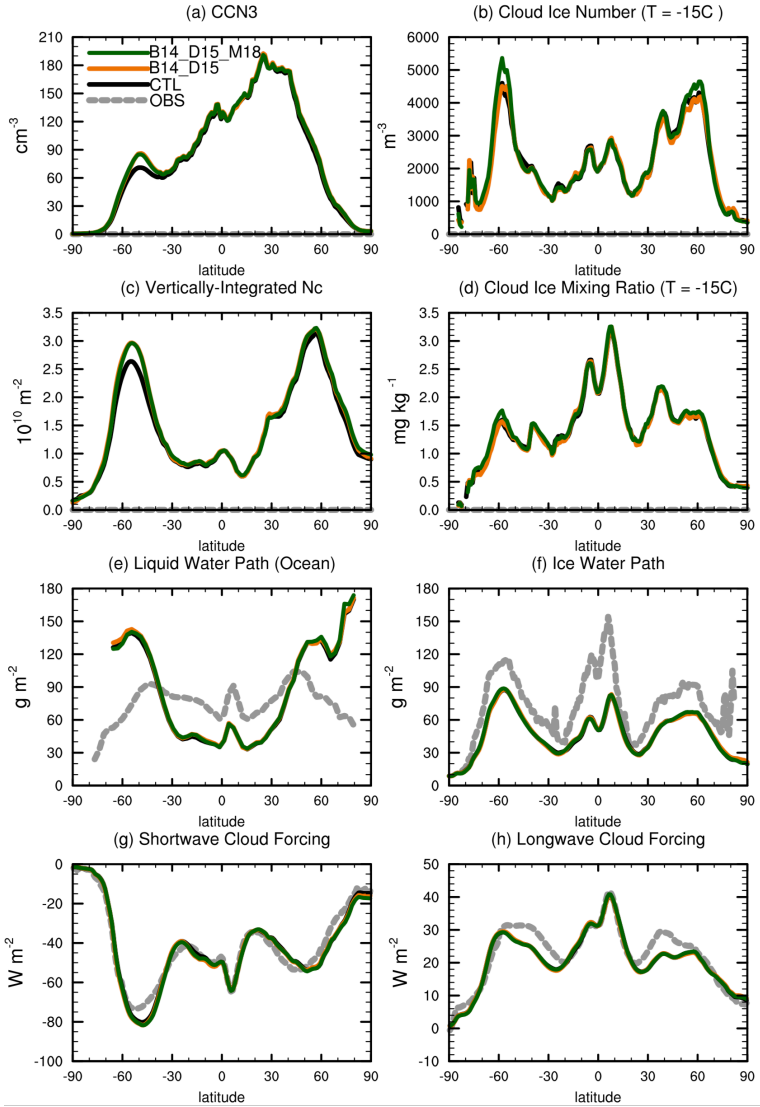

Figure 8. Annual zonal-mean distributions of (a) surface CCN concentration at S=0.1%, (b) cloud ice number concentration on T=–15°C isotherm, (c) vertically-integrated cloud droplet number concentration, (d) cloud ice mass mixing ratio on T= –15°C isotherm, (e) liquid water path over ocean, (f) ice water path, (g) shortwave cloud forcing, and (h) longwave cloud forcing for CTL (black), B14_D15 (orange), and B14_D15_M18 (green), along with available observations (gray dashed lines) as references. The –15°C isotherm level was selected in (b) and (d) to better represent the mixed-phase cloud feature.

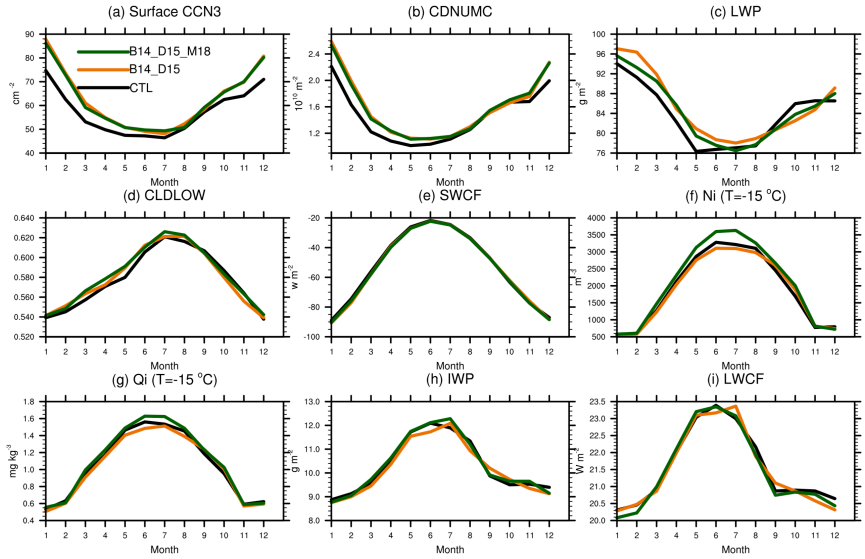

Figure 9. Seasonal cycle of (a) surface CCN at 0.1% supersaturation, (b) vertically-integrated cloud droplet number concentration, (c) liquid water path, (d) low cloud amount, (e) shortwave cloud forcing, (f) cloud ice number concentration on T= –15℃ isotherm, (g) cloud ice mass mixing ratio on T= –15℃ isotherm, (h) ice water path (IWP), and (i) LWCF, for CTL (black), B14_D15 (orange) and B14_D15_M18 (green).